General Disclaimer

One or more of the Following Statements may affect this Document

- This document has been reproduced from the best copy furnished by the organizational source. It is being released in the interest of making available as much information as possible.

- This document may contain data, which exceeds the sheet parameters. It was furnished in this condition by the organizational source and is the best copy available.

- This document may contain tone-on-tone or color graphs, charts and/or pictures, which have been reproduced in black and white.

- This document is paginated as submitted by the original source.

- Portions of this document are not fully legible due to the historical nature of some of the material. However, it is the best reproduction available from the original submission.

National Aeronautics and Space Administration

NASA TM-82477

George C. Marshall Space Flight Center
Marshall Space Flight Center, Alabama 35812

Spacelab Mission 2 Experiment Descriptions - Second Edition

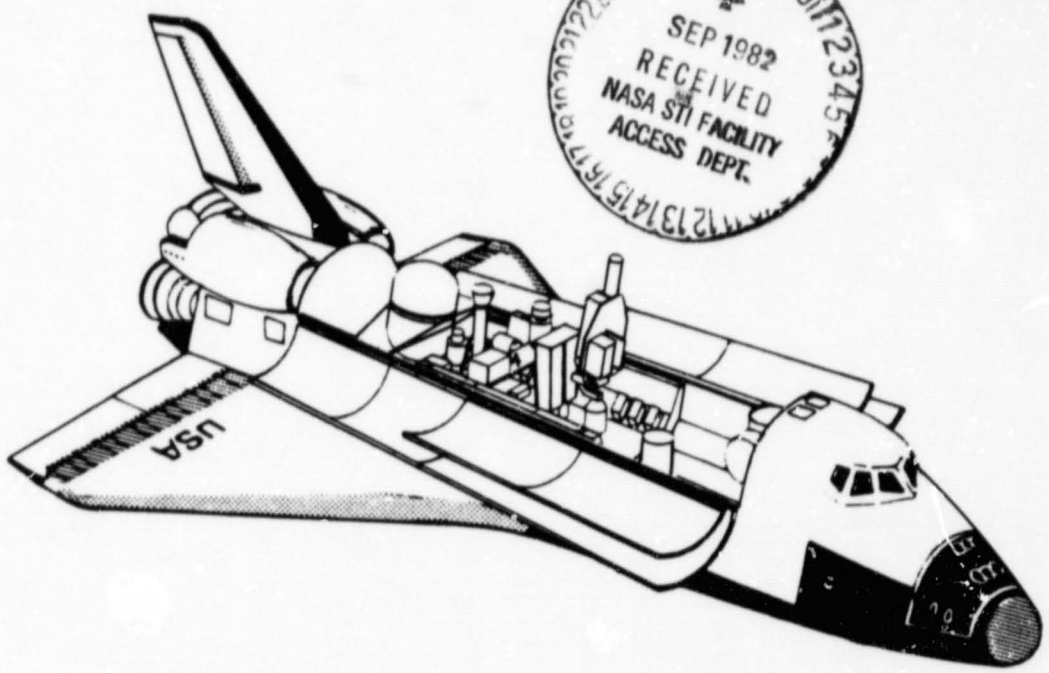

Edited by K. Stuart Clifton
Space Sciences Laboratory

January 1982

ACKNOWLEDGMENTS

The editor would like to express his gratitude to all the Principal Investigators and Co-Investigators who contributed to the experiment descriptions. He would also like to thank E. Weiler and E. Fleischman of NASA Headquarters for their support; E. Urban of MSFC for helpful comments and suggestions; and S. Davis, M. Durkee, and A. Tingle for their assistance.

FOREWORD

Spacelab 2 is the second in a series of modular orbiting laboratories to be undertaken in the 1980's. Spacelab is provided by the European Space Agency (ESA) and flown into space by the Space Transportation System developed by the National Aeronautics and Space Administration (NASA). The general Spacelab modules consist of unpressurized experiment pallets and pressurized modules which can be arranged in several combinations within the payload bay of the Space Shuttle Orbiter. Spacelab 2 is a pallets-only mission in which most of the experiments are operated from the Orbiter aft flight deck. The Spacelab 2 configuration is shown in Figure 1.

Overall management of the first three Spacelab missions is under the direction of the Office of Space Sciences and Applications at NASA Headquarters. The Marshall Space Flight Center (MSFC) has been assigned as the project management center for these Spacelab missions. Dr. Edward Weiler of NASA Headquarters has been designated the Program Scientist for Spacelab 2, and Dr. Eugene W. Urban of MSFC is the Spacelab 2 Mission Scientist.

Spacelab 2 is currently scheduled to be launched from the Kennedy Space Center (KSC) in November 1984 with a mission duration planned for 7 days. An orbital altitude of approximately 390 km will be achieved with an inclination of 49.5 degrees. The Shuttle will land at the Kennedy Space Center following the mission.

As with the first Spacelab mission, noncareer astronauts will be used on-orbit to conduct the scientific investigations. These astronauts, called Payload Specialists, are scientists selected and trained by the investigators developing the experiments to be flown on this mission. Four Payload Specialists have been chosen for the Spacelab 2 mission; two will fly aboard the spacecraft, and two will provide ground-based support. They are Dr. Loren Acton of the Goddard Space Flight Center, Dr. John-David Bartoe of the Naval Research Laboratory, Dr. Dianne Prinz of the Naval Research Laboratory, and Dr. George Simon of the Air Force Geophysics Laboratory. In addition to two Payload Specialists, the on-board crew will consist of a pilot, co-pilot, and two mission specialists, the latter charged with operation of Spacelab and Orbiter subsystems.

As with the first Spacelab mission, the primary objective of this mission is to verify the performance of Spacelab systems and subsystems, to determine the interface capability of the Spacelab and Orbiter, and to measure the environment induced by the spacecraft. The secondary objective of the mission is to obtain scientific and technology data and thus to demonstrate the capability of Spacelab to support multidisciplinary investigations.

Twelve investigations have been selected to participate in the Spacelab 2 mission. Of these, ten originate from the United States and two from the United Kingdom. The experiments represent a total of seven different disciplines, including life sciences, plasma physics, astronomy, high-energy astrophysics, solar physics, atmospheric physics, and technology research. Table 1 lists the experiments by experiment number, title, discipline, principal investigator, and sponsoring institution. A list of co-investigators, many of whom were also instrumental in the writing of the experiment descriptions, is provided in the Appendix.

Eight of the twelve experiments are located on three pallets in the payload bay. In addition, a special structure has been designed to support the cosmic-ray experiment. The physical location of these experiments is shown in Figure 2. The two life sciences experiments will be carried in the Orbiter mid-deck shown in Figure 3, and one experiment involves only observations from the ground.

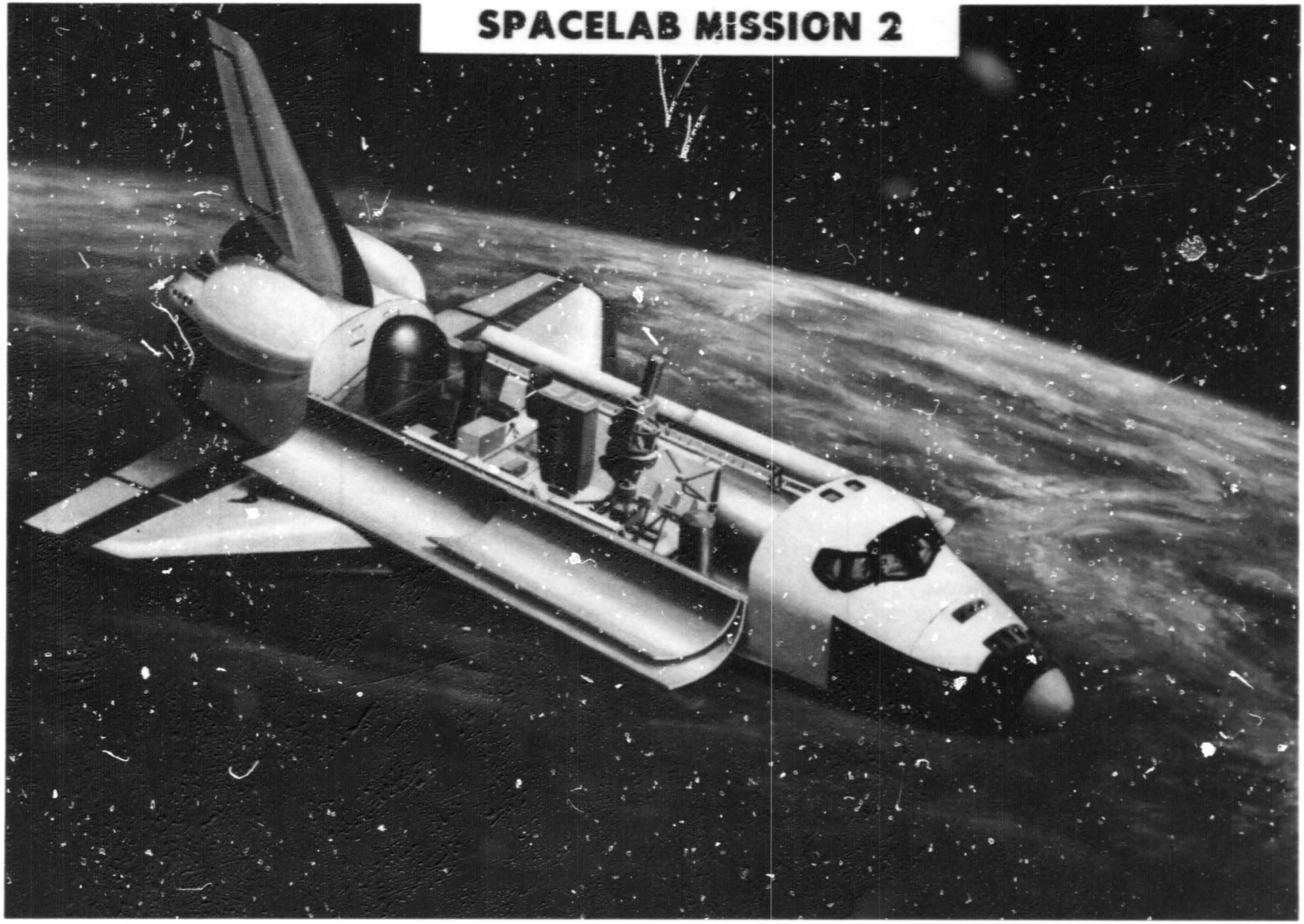

ORIGINAL PAGE
COLOR PHOTOGRAPH

Figure 1. Spacelab 2 and instrument complement.

TABLE 1. LIST OF SPACELAB 2 EXPERIMENTS

Discipline	Experiment Number	Title	Principal Investigator/Institution
Life Sciences	2SL-01	Vitamin D Metabolites and Bone Demineralization	H. K. Schnoes/University of Wisconsin
	2SL-02	Interaction of Oxygen and Gravity Influenced Lignification	J. R. Cowles/University of Houston
Plasma Physics	2SL-03	Ejectable Plasma Diagnostics Package	S. D. Shawhan/University of Iowa
	2SL-04	Plasma Depletion Experiments for Ionospheric and Radio Astronomical Studies	M. Mendillo/Boston University P. Bernhardt/Los Alamos National Laboratory
Infrared Astronomy	2SL-05	Small Helium-Cooled IR Telescope	G. G. Fazio/Smithsonian Astrophysical Observatory
High Energy Physics	2SL-06	Elemental Composition and Energy Spectra of Cosmic Ray Nuclei	P. Meyer, D. Müller/University of Chicago
	2SL-07	Hard X-Ray Imaging of Clusters of Galaxies and Other Extended X-Ray Sources	A. P. Willmore/University of Birmingham, England
Solar Physics	2SL-08	Solar Magnetic and Velocity Field Measurement System	A. M. Title/Lockheed Palo Alto Research
	2SL-09	Solar Coronal Helium Abundance Spacelab Experiment	A. H. Gabriel/Rutherford and Appleton Laboratory, England J. L. Culhane/University College, England
	2SL-10	Solar UV High Resolution Telescope and Spectrograph	G. E. Brueckner/Naval Research Laboratory
Atmospheric Physics	2SL-11	Solar UV Spectral Irradiance Monitor	G. E. Brueckner/Naval Research Laboratory
Technology	2SL-13	Properties of Superfluid Helium in Zero-G	P. V. Mason/Jet Propulsion Laboratory

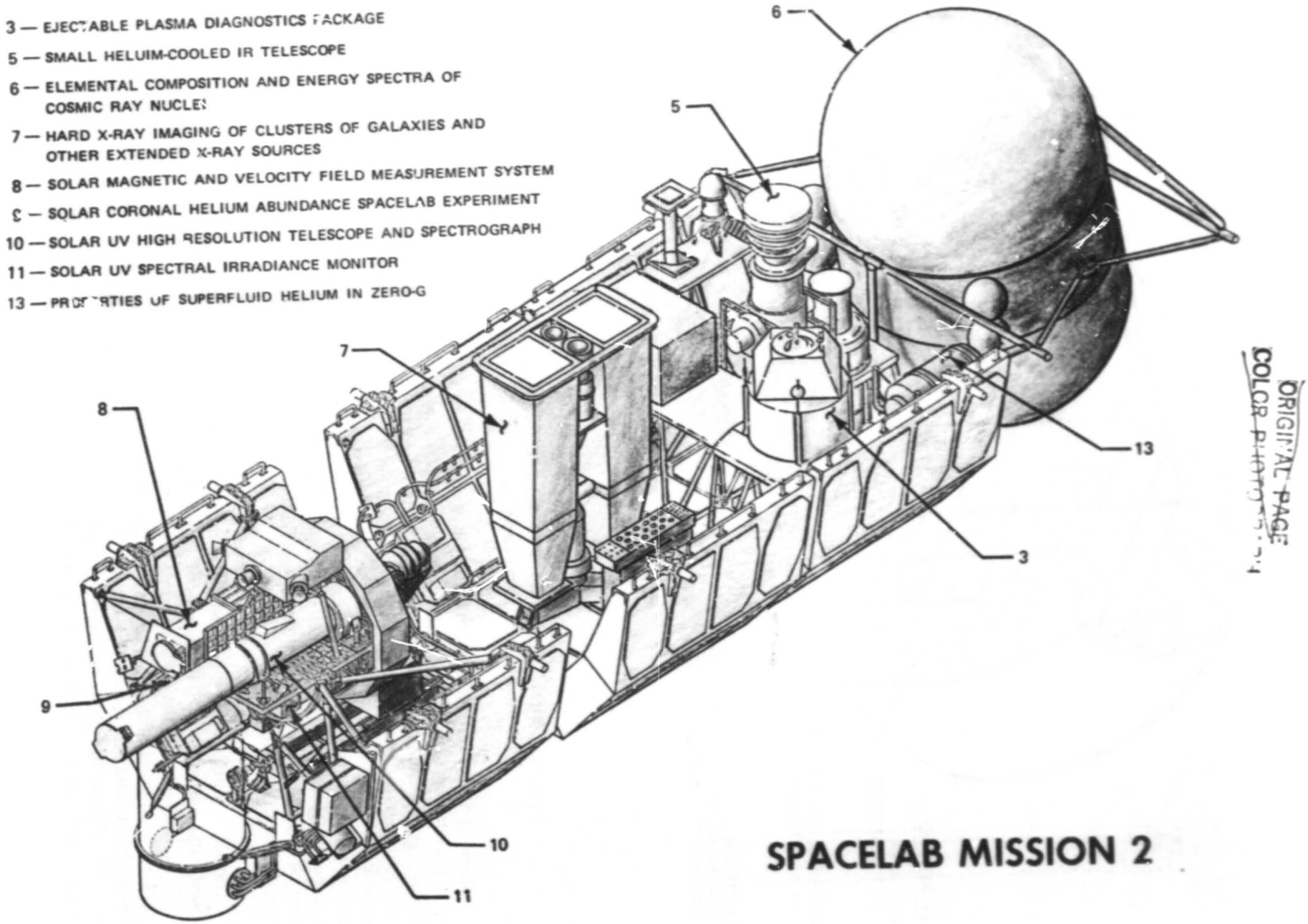

Figure 2. Spacelab 2 payload configuration indicating experiment location.

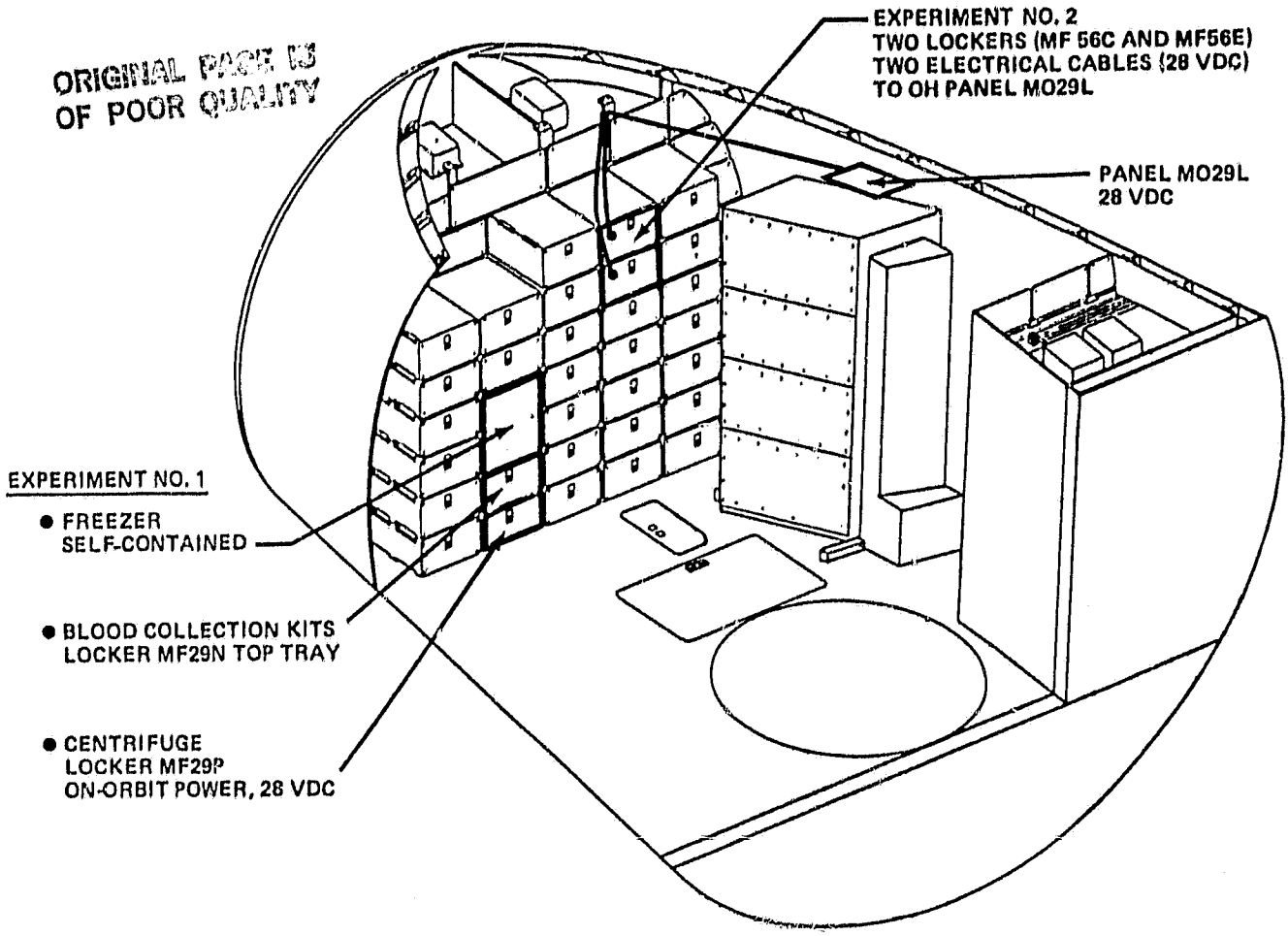

Figure 3. Orbiter mid-deck of Spacelab 2 showing storage of life sciences experiments (courtesy of Johnson Space Center).

Many of the investigations capitalize on the new capabilities of Shuttle and Spacelab. For example, the Orbiter's weight-carrying capacity allows the use of a massive instrument such as the cosmic-ray experiment (1968 kg), plus several other large instruments. The Plasma Diagnostics Package will demonstrate the use of the Remote Manipulator System, the capability of Orbiter to launch subsatellites, and the ability of the Orbiter to maneuver about the subsatellite in space. The solar-oriented experiments will utilize an Instrument Pointing System (IPS) developed by ESA. The IPS will accommodate the four experiments, which weigh a total of 717 kg, and will point them with an accuracy of 2 arc sec and with a quiescent stability of 1.2 arc sec. The current configuration of experiments on the IPS is shown in Figure 4.

The life sciences experiments will examine the effects of zero-gravity on the metabolism of both plants and animals. The formation of lignin in plant seedlings in a controlled oxygen environment will be studied, and the derangements of mineral metabolism in humans during prolonged spaceflight will be monitored. Plasma physics experiments will investigate the Orbiter's local electromagnetic environment and the interaction of the Orbiter with the magnetosphere from a deployed subsatellite. The Orbiter thrusters will also be used to create regions of electron depletion in the ionosphere which can be monitored from ground-based observatories.

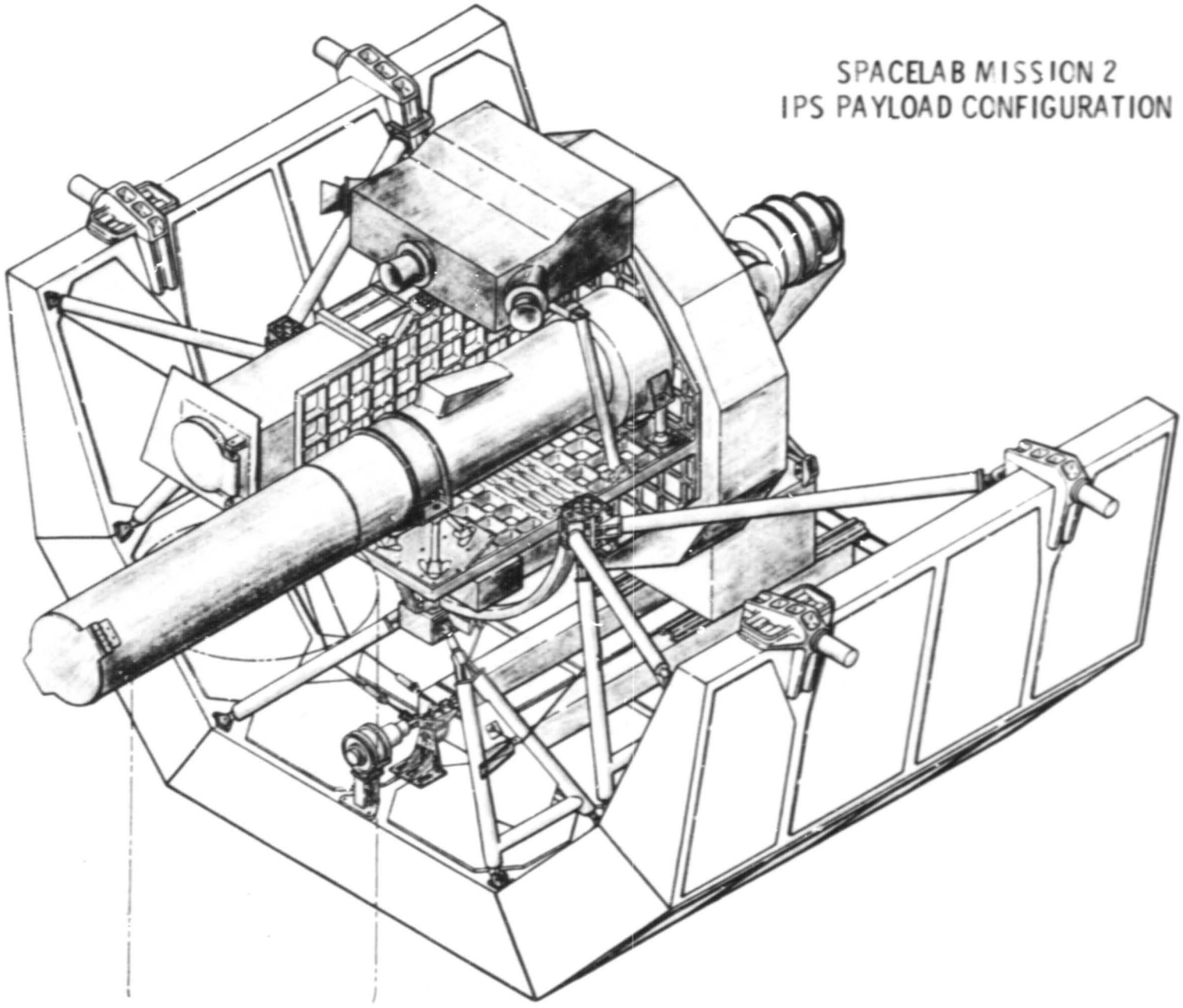

Figure 4. IPS configuration of solar experiments.

An infrared astronomy experiment will map spatially extended sources of infrared radiation over much of the sky. The results will complement studies of compact infrared sources being made at about the same time by the Infra Red Astronomical Satellite (IRAS). A high-energy experiment will determine the charge composition and energy spectra of cosmic-ray nuclei at energies previously unobservable from the ground. In addition, an X-ray telescope will be used to study X-ray emission from clusters of galaxies in an attempt to resolve emission mechanisms.

The solar physics experiments will include a study of small-scale solar magnetic and velocity field structures with high temporal and spatial resolution and a high-accuracy determination of the absolute abundances of helium in the solar corona. In addition, an examination will be undertaken with high spectral and spatial resolution of intensity fluctuations, Doppler shifts, and line profile changes which are crucial to the understanding of the mechanisms that are responsible for the heating of the chromosphere, transition zone, and corona. An atmospheric science experiment is aimed at establishing the total solar ultraviolet flux with high accuracy and its changes over a solar activity cycle.

The technology experiment will evaluate the use of Spacelab as a low-g test facility. In addition, the thermal and fluid properties of superfluid helium in zero-gravity will be examined as requisite for future space experiments using superfluid helium as a cryogen.

Although Spacelab 2 represents a multidisciplinary mission with experiments selected independently, a number of joint investigations are planned during the mission. Indeed, 8 of the 12 experiments on the SL2 mission are participating in different collaborative efforts. Complementary science goals have been developed between the Plasma Science experiments, between the X-ray Telescope and IR Telescope, and among the four IPS-Mounted Solar experiments.

The flight of Spacelab 2 represents a pioneering effort, and the results obtained from the mission will benefit a wide range of scientific inquiry. It will yield important insight into many of the physical processes occurring on Earth and in space and in this way establish another step in the basic understanding of the universe.

TABLE OF CONTENTS

LIST OF ILLUSTRATIONS

LIST OF ILLUSTRATIONS (Concluded)

I. VITAMIN D METABOLITES AND BONE DEMINERALIZATION
(2SL-01)

Heinrich K. Schnoes
University of Wisconsin

Medical and physiological examination of crew members of the Gemini, Apollo, and Skylab missions has demonstrated a pattern of bone mineral loss, increased urinary calcium, and significant losses of phosphorus and nitrogen. The general medical picture rather closely resembles the symptoms exhibited by long-term, bed-rested or otherwise immobilized and physically inactive subjects on Earth. Although the effect of relatively short-term exposure to a gravity-free environment on mineral balance does not seem as pronounced and significant as originally feared, bone mineral depletion and phosphorus and nitrogen losses are clearly real phenomena, and the severity of symptoms appears directly correlated with duration of exposure to the zero-g environment. This lack of eventual adaptation of the organism to the gravity-free milieu points to mineral loss as a potentially serious medical consequence of prolonged space habitation, and this concern, as well as the common occurrence of the same problem under certain terrestrial conditions, suggests that the detailed investigation of biochemical agents potentially involved in the control or modulation of the process will represent a scientifically rewarding endeavor yielding results of considerable practical significance.

This experiment, as a contribution toward an understanding of the molecular basis of bone demineralization and mineral imbalance and increasing fecal calcium under conditions of prolonged space flight, will measure quantitatively the blood levels of biologically active vitamin D metabolites of flight crew members of the Spacelab 2 mission. This work is intended to establish whether these derangements of mineral (specifically calcium) metabolism reflect themselves in any way in a modulation of vitamin D metabolism to its various metabolites. During the past decade, research into the biochemistry of vitamin D has established that these vitamin metabolites are key agents in the maintenance of calcium and phosphate homeostasis. Since the biosynthesis of D-metabolites is subject to regulations by several physiological parameters, the monitoring of these metabolites under normal and zero-g conditions can be expected to yield important insights into the molecular aspects of the homeostatic mechanism in a gravity-free milieu. These metabolite levels are to be determined by established methods such as competitive protein binding, high-pressure liquid chromatography, and gas-liquid chromatography, as well as by new, very general and highly sensitive techniques to be further developed as part of the program. Since bone mineral loss is a phenomenon not unique to the space environment, but is observed also under certain terrestrial conditions, the results would also be relevant to musculoskeletal research in general, and any treatment methods could find broad application in normal medical practice. Furthermore, the successful development of rapid and convenient analytical methods for metabolite assay would be of very great benefit to clinical research toward an understanding and control of a variety of calcium metabolism disorders, such as osteoporosis, osteodystrophy, vitamin D resistant rickets, hyper- and hypoparathyroidism, and others.

The experiment is composed of two phases: a developmental phase and a final phase. As part of the developmental phase, existing analysis methods for the vitamin D metabolites will be refined and new methods developed. Experimental protocols will be tested using samples from animal and human experiments. Plasma from animals, e.g., rats, chickens, and monkeys, maintained on diets differing in vitamin D supplementation and with motion restricted (simulated weightlessness), collected at different intervals during the day will be assayed. Human specimens derived from normal, diseased subjects (particularly those with liver, kidney, or bone related problems), and bed-rested patients will

complement the animal work. These studies should give a diversity of samples which allow: (1) definition of the most effective and appropriate methods for analysis of the vitamin D metabolites in plasma samples of the flight crew, (2) definition of the optimum experimental protocol, and (3) acquisition of an extensive set of baseline data.

The final phase will consist of the quantitative analysis of the vitamin D metabolites in plasma samples of the Spacelab 2 crew collected prior to, during, and postflight. During flight operations, a specimen collection of 25 ml of anticoagulated blood from each of the five crew persons will be made once early and once late in the mission. The plasma will be separated from the blood cells by centrifugation and stored in a freezer (-20°C) for the remainder of the flight. Upon return to Earth, the frozen plasma will be analyzed.

The flight experiment hardware (Fig. I-1) will consist of two blood collection kits, a centrifuge to prepare the plasma, and a -20°C freezer for sample storage. All of the equipment will be located in the Orbiter mid-deck. The physical characteristics of the flight experiment are shown in Table I-1.

TABLE I-1. PHYSICAL CHARACTERISTICS

Dimensions:
Blood Collection Kits (2): 44 X 25 X 8 cm (Mid-Deck)
Centrifuge: 39 cm Dia X 19 cm (Mid-Deck)
Freezer: 51 cm Dia X 24 cm (Mid-Deck)
Total Mass: 32 kg
Average Power: 200 W at 260 V, 3 ϕ, 400 Hz
Total Energy: 0.3 kWh
Data: Returned Samples

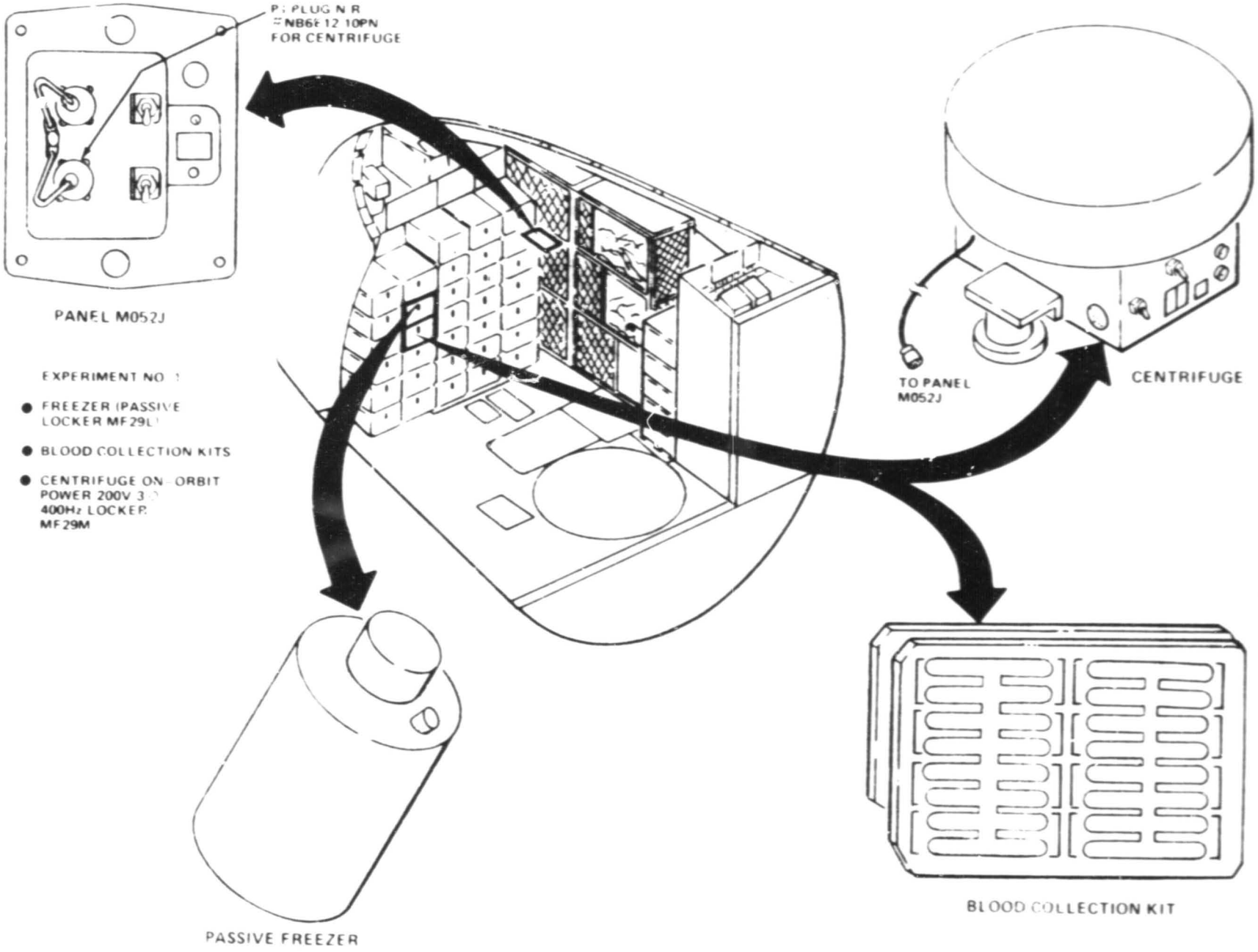

Figure I-1. Flight hardware for metaboiism experiment (not shown to scale).

II. THE INTERACTION OF OXYGEN AND GRAVITY-INFLUENCED LIGNIFICATION (2SL-02)

Joe R. Cowles
University of Houston

This experiment is part of a general program of research on the regulation of lignification in higher plants and is designed to provide data on the mechanism of gravity reception in plants and the gravity-influenced lignin synthesis.

Lignin is a cross-linking polymer found in the walls of plant cells and is needed to provide strength and rigidity for plants in the terrestrial environment. While lignin is a valuable structural polymer, it has some undesirable qualities. Because lignin is difficult to degrade, its presence in food plants reduces overall digestibility. Lignin also interferes with the direct usability of industrially important cellulose from plants.

A significant portion of the metabolic carbon derived from photosynthesis is channeled into lignin synthesis. It is the second most abundant carbon compound in nature, comprising up to 30 percent of some plant tissues. Since metabolic energy is required for lignin synthesis, the synthesis of large amounts of lignin can divert photosynthate from synthesis of more digestible materials, such as proteins, lipids, and carbohydrates. Therefore, while a certain amount of lignin is necessary in plants, the ability to control the process and to affect its synthesis would be of considerable benefit to man.

Since gravity is believed to be a primary controlling stimulus for lignification, especially in gymnosperms, a weightless environment offers an excellent tool for testing certain hypotheses concerning the mechanism of lignin formation. For example, how is lignin synthesis influenced by gravity? Furthermore, weightlessness allows for the removal of gravity as a factor in controlling plant growth and development. Of particular interest in this experiment is the observation that the quantity of lignin in plant tissues is significantly altered by oxygen. The use of the weightless environment eliminates the effect of gravity upon lignification and, thus, separates this effect from other controlling factors such as oxygen concentrations.

The objective of this experiment is to determine the effect of weightlessness upon lignification and to establish the overall effect of oxygen on lignin formation independent of any gravity effects.

The experiment is an integral and essential aspect of a broadly based study aimed at the elucidation of the nature of the gravity receptor, the mechanism of gravity mediation of lignification, the regulation of lignification, and the alternative influence on other aromatic pathways in higher plants.

The experiment involves the exposure of developing plant seedlings to two different oxygen concentrations in the nominal weightless conditions of orbital flight. Young pine seedlings will be planted in metabolic chambers just prior to launch. The chambers will be sealed and the atmospheric composition brought to desired levels by flushing the chambers with known gas mixtures. One oxygen concentration will be 21 percent (control) and the other 10 percent or less. Each oxygen concentration will be duplicated. The plant growth unit (PGU) is fitted with lamps programmed for day/night cycles. At the latest possible time before launch, the PGU will be carried on board and installed in a mid-deck locker of the Shuttle Orbiter. The PGU is self-contained and the experiment will fly passively. The experiment also will be duplicated on the ground at 1 g (control).

Within 1 hr after landing, the PGU will be removed as a carry-off item. The atmosphere of the chambers will be sampled and analyzed for metabolic gases. The seedlings will be photographed, measured, and processed for analysis. The tissue sections will be analyzed with respect to the rate of lignin development, quantities of lignin produced, and activities of selected enzymes in the lignin biosynthetic pathway. The results between flight and ground-control tissues will be compared and reported.

The physical characteristics of the flight package are shown in Table II-1.

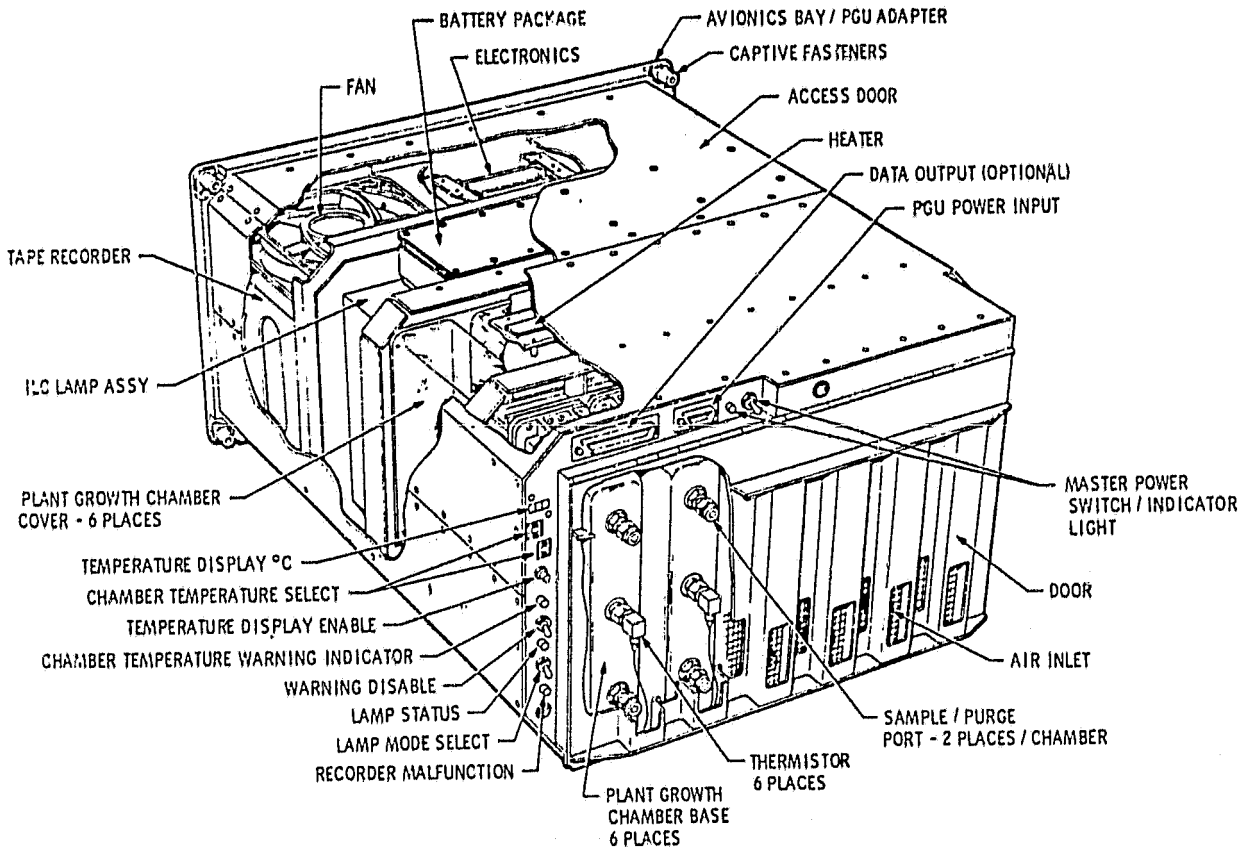

Figure II-1. Experiment 2 (2SL-02) carry-on lignification experiment.

TABLE II-1. PHYSICAL CHARACTERISTICS

Dimension: 51 X 36 X 27 cm (Mid-Deck)
Total Mass: 24 kg
Average Power: 52 W at 28 Vdc
Total Energy: 9 kWh
Data: Returned Samples

III. AN EJECTABLE PLASMA DIAGNOSTICS PACKAGE (2SL-03)

Stanley D. Shawhan
The University of Iowa

The motion of the large, partially conducting, partially insulated Orbiter through the magnetized ionospheric plasma offers the basis for an "active" plasma experiment when coupled with a co-orbiting set of plasma diagnostics instrumentation. Because of its size, the Orbiter can develop significant potentials on its surface from the motional electric fields. For the conducting parts of the Orbiter, these electric fields will cause current systems in the plasma which may produce a variety of plasma instabilities leading to electrostatic waves and accelerated thermal particles. Charges will build up on the insulating surfaces, which offers the opportunity to study spacecraft charging effects. Also, the Orbiter is many ion gyroradii in size so that it will produce a significant ion ram (aerodynamic) wake which may also result in the production of waves and in the alteration of the total electron density and temperature.

Many of these plasma interaction phenomena cannot be studied from instruments on the Orbiter itself because of electromagnetic interference levels and because the phenomena may exist only away from the Orbiter, such as in the wake region. However, such phenomena could be investigated using an ejectable subsatellite fully instrumented to detect thermal and energetic particles, electrostatic and electromagnetic waves, and electric and magnetic fields associated with these interactions. Furthermore, the unique capability of the Orbiter to maneuver about the subsatellite would provide the necessary spatial sampling of the active Orbiter's induced wave particle environment.

The Plasma Diagnostics Package (PDP) is such a fully instrumented, ejectable subsatellite. During the Spacelab 2 mission it will operate within the payload bay, on the Remote Manipulator System (RMS), and as a free flyer. Its objectives are: (1) to study Orbiter-magnetoplasma interactions in terms of density wakes, dc electric fields, energized plasma, and a variety of possible wave-particle instabilities; (2) to provide in situ measurements of the ionospheric plasma "holes" induced by the Orbiter engine burns in support of the ground radar observations of Spacelab 2 Experiment 4 (2SL-04); (3) to measure fields, waves, and plasma modifications induced by the Orbiter/Spacelab operating systems in the Spacelab bay and out to distances of 10 km; (4) to observe natural waves, fields, and plasmas in the unperturbed magnetosphere; (5) to assess the Spacelab system for performance of active and passive magnetospheric experiments; and (6) to develop the methods and hardware to operate instruments at the end of the remote manipulator arm and to eject small scientific subsatellites.

Instruments mounted within the PDP to achieve these objectives include: (1) a quadrispherical low energy proton and electron differential analyzer for measurement of nonthermal electron and proton distribution functions from 2 eV to 25 KeV with sufficient resolution that isolated features can be studied in detail; (2) a plasma wave analyzer/electric dipole and magnetic search coil sensors to measure the components of electromagnetic and electrostatic waves from 5 Hz to 2 GHz; (3) a dc electric field meter for sensing components of the dc electric field over the range from 2 to 2000 mV/m; (4) a triaxial flux-gate magnetometer to measure the dc magnetic field distribution in the vicinity of the Orbiter; (5) a Langmuir probe to measure electron density in the region 10^3 to 10^7 cm^{-3} and electron temperature from 500 K to 5000 K; (6) a retarding potential analyzer and differential flux analyzer to determine the energy distribution and streaming velocity direction for plasma

ions and energies <16 eV, number densities of 2 X 10 to 10^7 cm^{-3}, temperatures of 500 to 10^6 K, and velocities up to 15 km/s within ±50 degrees of the instrument spin plane: (7) an ion mass spectrometer for 1 to 64 AMU at densities of 20 to 2 X 10^6 cm^{-3}; and (8) a cold cathode vacuum gauge for 10^{-3} to 10^{-7} torr.

In addition the PDP, the experiment consists of a Special Purpose End Effector (SPEE), a Release Mechanism (REM), a Receiver and Data Processing (RDP) assembly, and an RF Antenna (RFA) assembly. A schematic of the experiment hardware is shown in Figure III-1. The SPEE provides the mechanical and electrical interface between the PDP and the RMS. Once attached to the RMS, via a grapple fixture compatible with the RMS standard end effector, the SPEE provides control of a few PDP functions and serves to spin up the PDP to approximately 6 rpm before releasing it from the arm. The REM is hardmounted to the pallet and serves to support mechanically the PDP and SPEE assembly for launch and the SPEE for landing. The RDP which controls and monitors the PDP prior to RMS operations is mounted separately on a cold plate. The RDP also contains a microprocessor, the RF receiver for demodulating the PDP telemetry, and assorted electronics. The RFA consists of a fixed mast and a flat-plate, dual-polarized antenna to receive the 400 MHz telemetry data from the PDP. The physical characteristics of the experiment are listed in Table III-1.

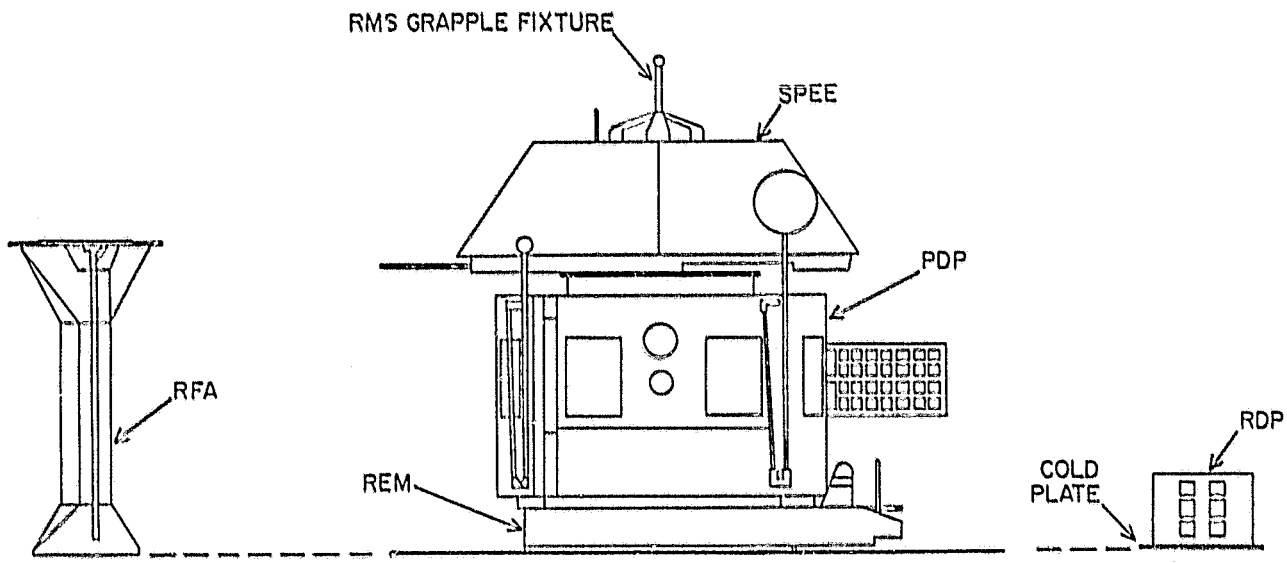

Figure III-1. Plasma Diagnostics Package and associated equipment.

TABLE III-1. PHYSICAL CHARACTERISTICS

Dimensions:
- Plasma Diagnostics Package: 112 cm Dia X 85 cm
- Special Purpose End Effector: 93 X 93 X 40 cm
- Release Mechanism: 120 X 120 X 16 cm
- RF Antenna Assembly: 40 X 40 X 85 cm
- Receiver and Data Processing Box: 33 X 50 X 20 cm

Total Mass: 383 kg

Average Power: 34 W at 28 Vdc

Total Energy: 4.53 kWh

Data: Digital: 320 kbps; Video: 4.2 MHz

Operations of the PDP will commence with the instrument mounted in the payload bay to monitor the changes in electric and magnetic field strengths from dc to 2 GHz as different Orbiter subsystems and other experiments are activated. The PDP is then attached to the RMS via the SPEE, as shown in Figure III-2, and positioned along a sequence of predetermined points within the Orbiter bay to locate sources of EMI, and at points along the wings and cockpit to examine plasma sheath phenomena. At times the PDP will be brought to within 2 m of Orbiter surfaces and assemblies. While attached to the RMS, the PDP will also search for Orbiter-induced shocks and wakes within the immediate vicinity of the Orbiter.

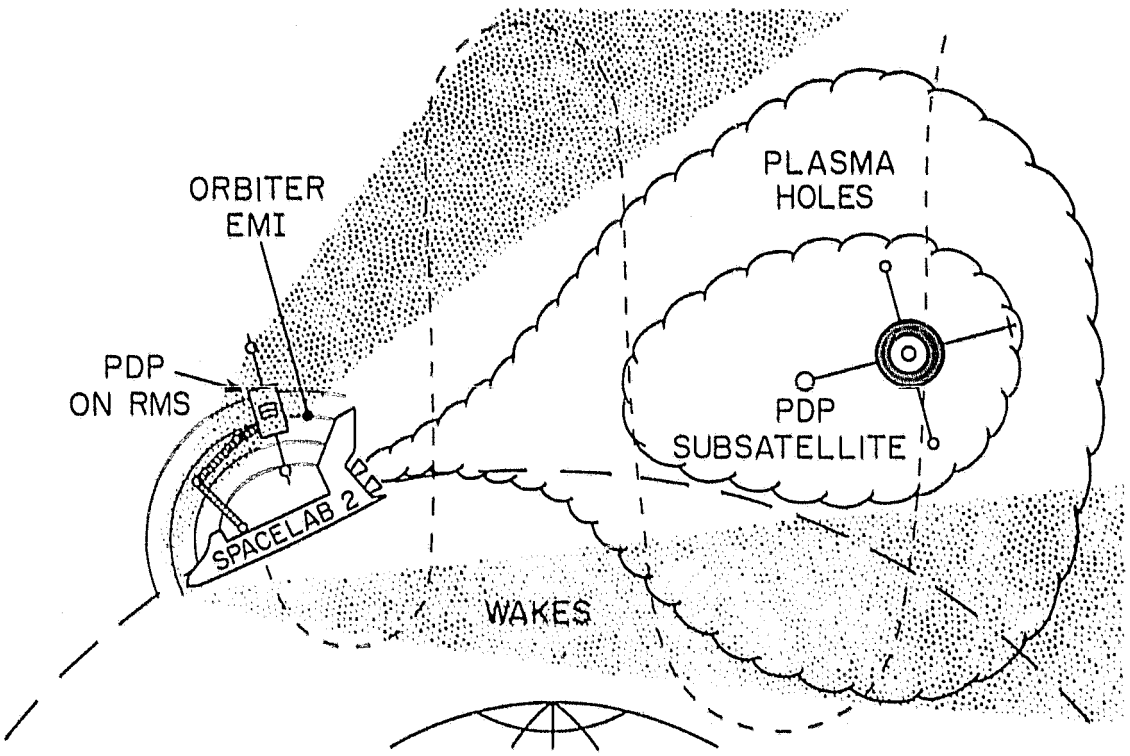

Figure III-2. Orbiter hardware PDP maneuvers.

Measurements of wake effects induced by the Orbiter will be made at low latitudes, particularly in the equatorial regions when the velocity vector is nearly along the magnetic field lines. The Orbiter will be maneuvered as shown in Figure III-2 to obtain PDP transits through its aerodynamic wake at distances varying from 50 m to 10 km.

In a coordinated effort with Experiment 2SL-04, Plasma Depletion Experiments for Ionospheric and Radio Astronomical Studies, the PDP subsatellite will make in situ measurements of the plasma depletion phenomena resulting from the burns of the Orbital maneuvering system over selected targets.

The PDP will then be released from the RMS at a separation velocity slightly less than 4 m/min. As it moves to a distance of approximately 100 m, the PDP will monitor EMI levels as a function of distance from the Orbiter. At the 100-m range, the Orbiter will be rotated sequentially about two axes to obtain a crude map of the angular distribution of EMI fields.

In addition to the study of Orbiter-induced effects, the PDP will also obtain measurements of natural magnetospheric and ionospheric phenomena such as aurorae, very low frequency (VLF) waves, magnetic substorms, and F-region plasma bubbles, as well as the persistent effects of the Orbiter water releases and thruster firings.

The PDP will also be used with reduced objectives as a part of the OSS-1 payload aboard STS-3, an earlier Shuttle mission flown in 1982. The configuration of the PDP for that mission is shown in Figure III-3.

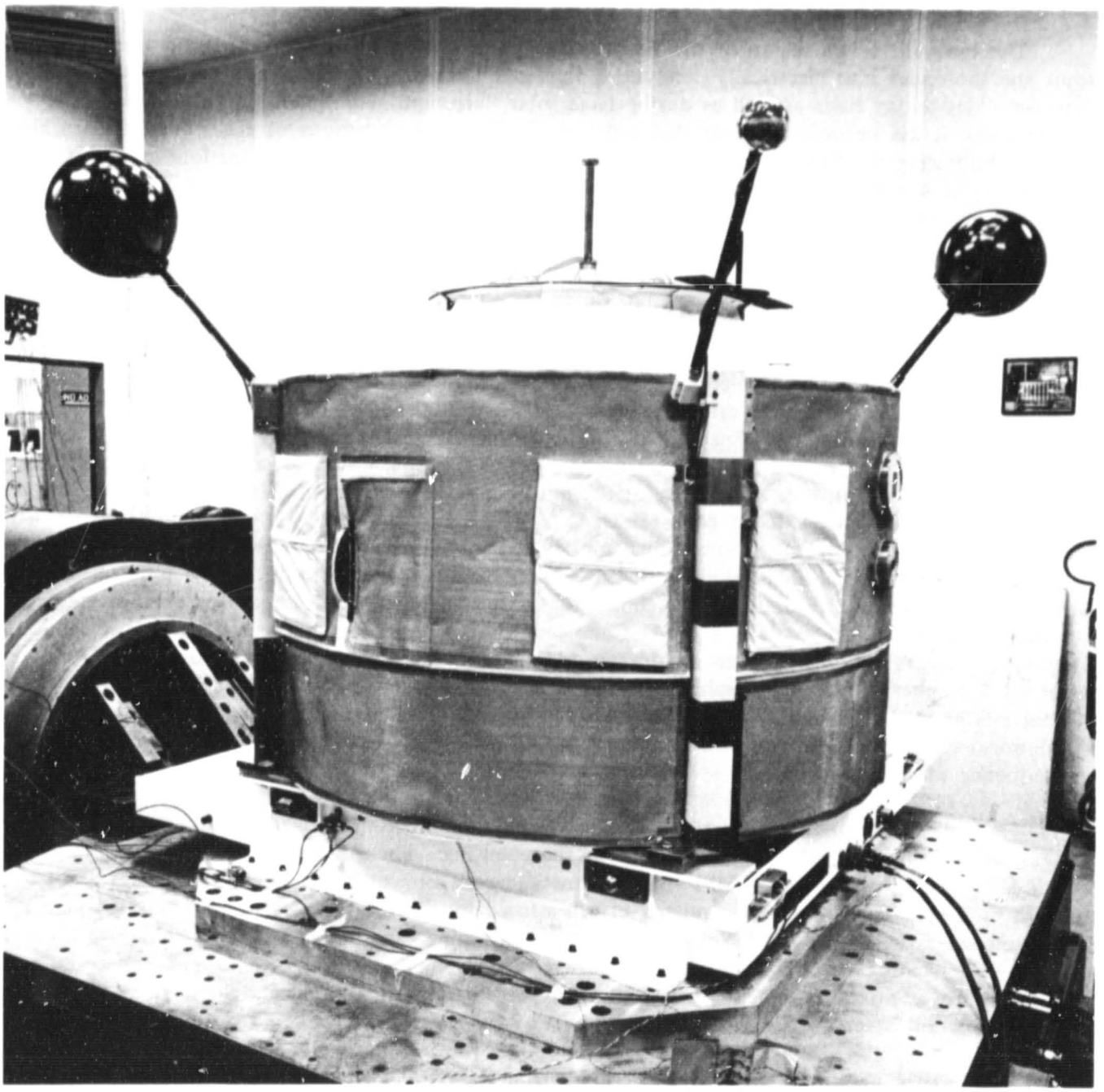

Figure III-3. OSS-1 configuration of Plasma Diagnostics Package during vibration testing.

IV. PLASMA DEPLETION EXPERIMENTS FOR IONOSPHERIC AND RADIO ASTRONOMICAL STUDIES
(2SL-04)

Michael Mendillo
Boston University

and

Paul Bernhardt
Los Alamos National Laboratory

The ionosphere is a region of the Earth's upper atmosphere where solar radiation transforms atoms and molecules into electrically conducting ions and electrons. Variations in the ionosphere occur on a day-to-day basis as well as during large solar flares and geomagnetic storms. During the past 20 years, it has become apparent that artificially induced perturbations of the ionosphere are also possible. Following the Skylab launch by a Saturn V rocket in May 1973, routine ionospheric measurements using satellite beacon techniques revealed that a large-scale ionospheric "hole" appeared along the east coast of the United States. The disturbance reduced the total electron content of the ionosphere by over 60 percent in magnitude, extended over an area exceeding 1000 km in radius, and lasted 2 to 4 hr. Analyses of the event indicated that the plasma depletions resulted from exceptionally enhanced chemical recombination rates between the ions and electrons caused by the molecular hydrogen and water vapor contained in the Saturn V second stage exhaust plume.

The Spacelab-2 Plasma Depletion Experiments for Ionospheric and Radio Astronomical Studies are designed to repeat the Skylab effect under controlled circumstances, using the Space Shuttle as the source of the perturbations. Specifically, the experimental goal is to study the ionospheric depletions and related effects caused by the exhaust gases from the Space Shuttle propulsion systems firing in the 300- to 500-km altitude range, i.e., in the midst of the "ionospheric F-layer." Many of the constituents of the Shuttle exhaust gases (H_2O, CO_2, H_2, etc.) react rapidly with the F-layer's oxygen ions (O^+) to produce polyatomic ions which rapidly recombine with the ambient electrons (e^-). Thus, the overall effect of chemical reactions with the exhaust vapors is a local reduction in ionospheric plasma concentrations. Calculations have shown that a release of 100 kg or more of exhaust gases into the F-layer will: (1) result in a marked and long-lasting depression in the electron concentration, (2) produce observable enhancements in airglow, (3) cause an electron temperature rise, and (4) create perturbed ionospheric and protonospheric regions which will affect radiowave propagation. Such induced effects might also be sufficient to assess the possibility of performing low-frequency radio astronomical studies from ground-based antennas for which the effective range is limited by the cut-off frequency of the ionosphere.

The concept behind the Spacelab 2 Plasma Depletion Experiments is to use the Space Shuttle itself as an experimental probe in a laboratory-in-space setting. Each of the experimentally dedicated Orbital Maneuvering Subsystem (OMS) engine burns addresses one or more specific objectives: (1) to study the ionospheric depletion and related effects caused by Shuttle thruster firings at midlatitudes; (2) to determine the nature of the physical processes governing ionospheric structure, including diffusion coefficients, chemical reaction rates, neutral wind velocities, electric fields, electron cooling rates, and limiting fluxes; (3) to produce controlled perturbations in the plasmasphere to examine the possible formation of artificial propagation paths for very low frequency (VLF) radio waves; (4) to test the artificial creation of a plasma instability responsible for ionospheric irregularities in equatorial regions; and (5) to use the ionospheric depletion region to conduct ground-based, high-resolution radio astronomical studies.

During flight operations, Shuttle thruster firings of the OMS will release from 130 to 1300 kg of exhaust vapors over each of several prescribed points along its orbit. Observations of the resulting plasma depletion regions will be made from ground-based sites selected for their location and their available instrumentation. The observatories to be used in the experiments are located in Westford, Massachusetts (USA); Roberval, Quebec (Canada); Arecibo (Puerto Rico); Kwajalein Island (Pacific Ocean); and Hobart, Tasmania (Australia). These observatories are indicated in Figure IV-1.

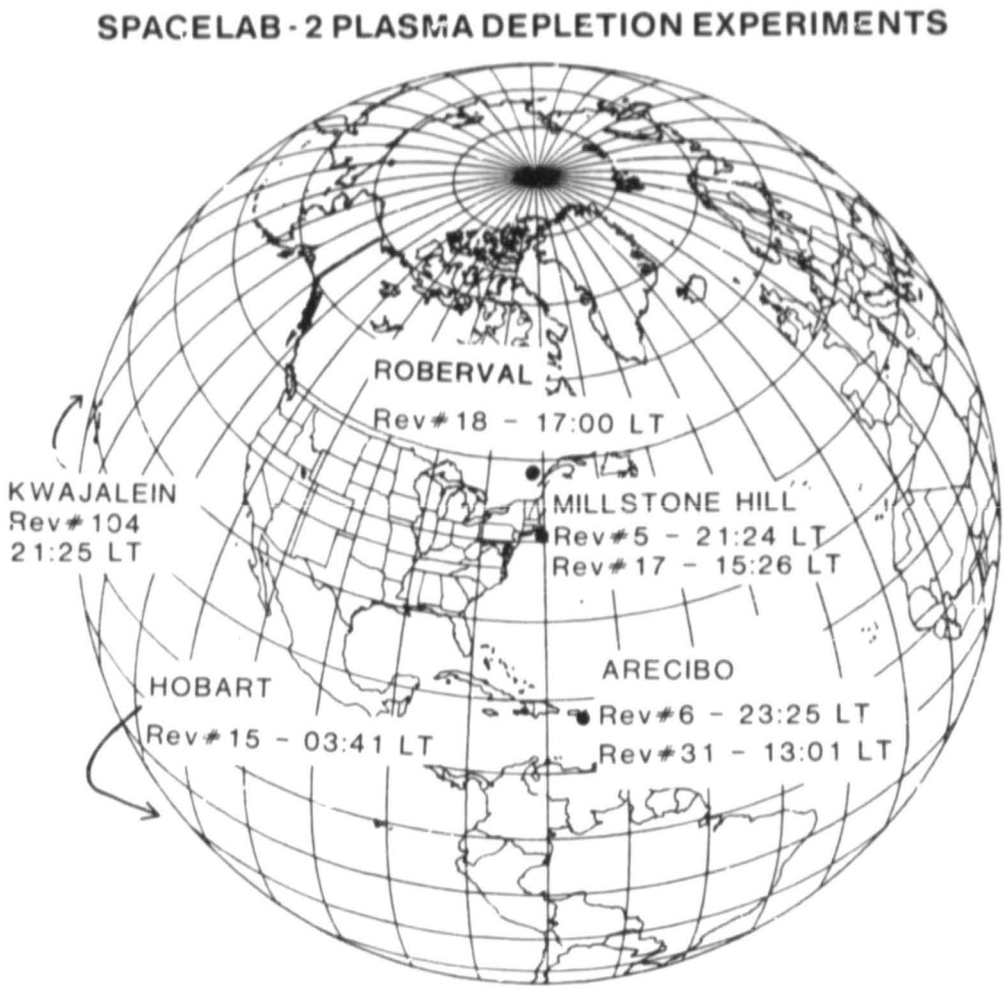

Figure IV-1. Observing sites for OMS burns giving Orbiter revolution number and local time for thruster firing.

High-midlatitude ionospheric hole measurements will be conducted at the Millstone Hill Incoherent Scatter Ionospheric Observatory in Westford, Massachusetts, during the 2-min engine burn required for circularization of the Shuttle's orbit. Reductions in electron concentrations, large-scale induced plasma drifts, and airglow emission will be measured during this nighttime experiment using the incoherent scatter radar technique with a 150-ft, fully steerable antenna. In addition, photometers and low-light-level television and 35-mm camera systems will make optical measurements of the airglow. Electron content and radio amplitude scintillation measurements will also be conducted using signals for geostationary satellites. A subsequent daytime experiment will be carried out using 150 kg of OMS thruster exhaust to study electron temperature enhancement effects.

Low-midlatitude measurements will be conducted at the National Astronomy and Ionospheric Center, Arecibo, Puerto Rico. The 1000-ft incoherent scatter radar at Arecibo Observatory will be used to measure perturbations in the electron density, ion composition, electron and ion temperatures, and plasma fluxes after the release of the exhaust vapors from the Shuttle engines. Daytime and nighttime experiments will be conducted over the Arecibo antenna. Temperature fluctuations and ion density reductions will be detected by radar and by optical means. Electron content measurements will be made from satellite signals passing through the modified region.

VLF propagation effects will be examined over Roberval, Quebec. The VLF propagation circuit between Roberval and Siple Station, Antarctica, will be used to measure the effects of artificially produced F-region gradients on the ionospheric propagation of VLF signals during the late afternoon hours. The ionospheric depletion will be transmitted up magnetic field lines and may form a protonospheric duct capable of trapping VLF waves. The measurements will involve Siple transmissions to Roberval and the reception at Siple of natural whistlers generated near Roberval. Electron content measurements will be conducted using polarimeters in conjunction with a geostationary satellite beacon. Optical observations may also be conducted.

The Shuttle engine burns over Roberval and Arecibo (day) will allow for the first simultaneous ground-based/sub-satellite study of ionospheric holes. The timing and magnitude of the OMS burn over Roberval were chosen to permit the Plasma Diagnostic Package (PDP, Experiment No. 3), while fixed to the manipulator arm in the cargo bay, to pass through the affected region approximately 90 min after the burn. Remote sensing of the ionosphere over Roberval will be made by the Millstone Hill radar throughout this period. Approximately 20 hr later, the PDP (now in free-flying mode 10 km behind the Orbiter) will be able to pass through the early phase of the daytime OMS burn over Arecibo. The coordination of these two experiments should yield as unique an "active space plasma experiment" as yet planned for the Shuttle.

The creation and study of artificially induced irregularities in the equatorial ionosphere will be undertaken using the ALTAIR and TRADEX Incoherent Scatter Observatories on Kwajalein Island in the Pacific. Kwajalein is located near the geomagnetic equator where ionospheric holes are unstable and tend to rise because of a Rayleigh-Taylor type gravitational instability. The Kwajalein radars, supported by optical transionospheric measurements, will be used to monitor the F-layer modification. The radars will provide backscatter information from which electron densities, vertical drifts, and plasma temperatures may be determined. Optical measurements will provide information concerning low-latitude neutral wind velocities, electric fields, and depletion morphology. Geostationary satellite radio beacon signals will be used to detect the presence of irregularities by monitoring scintillations in the received signals.

Low-frequency radio astronomy observations will be carried out over the low-frequency radio astronomical facilities of the University of Tasmania in Hobart, Tasmania, Australia. The University of Tasmania and the Reber antennas will be available for these measurements. The objective of the experiment will be to make low-frequency radio astronomical observations through a depleted duct in the ionosphere. These observations will attempt to measure the galactic radio noise in the 1 to 5 MHz range, where the peak of the galactic emission occurs. The experiment will also try to measure the focusing of radio waves by the ionospheric hole. Success in the experiment will imply that the use of artificial ionospheric windows and large ground-based antennas should allow one to obtain high-resolution observations in the 1 to 5 MHz range of different regions of the galaxy and to study several radio sources, such as the Vela and Gum Nebula, in the low-frequency domain. The Hobart experiment will also be monitored using ionospheric radio systems and optical diagnostic techniques. The OMS burn over Hobart is scheduled for the pre-dawn period in order to take advantage of the lowest possible background densities.

V. A SMALL, HELIUM-COOLED INFRARED TELESCOPE (2SL-05)

Giovanni G. Fazio
Smithsonian Astrophysical Observatory

This experiment is a joint program effort between the Smithsonian Astrophysical Observatory, the University of Arizona, and the NASA/Marshall Space Flight Center. The NASA/Ames Research Center will be associated with the experiment for induced contamination studies.

This experiment is multidisciplinary in nature, involving scientific and technical goals. Astronomical objectives will emphasize the study of diffuse emission and extended sources in the infrared sky, including:

a) The measurement and mapping of extended low surface-brightness infrared emission from the galaxy. Extended far infrared radiation from the galaxy was discovered in 1968 and has subsequently been measured over 50 degrees of galactic longitude to a surface brightness of 1×10^{-11} W/cm^2/ster at 100 μ. The sensitivity expected with the Spacelab 2 experiment, however, is more than 500 times more sensitive than current balloon experiments at 100 μ and will make possible an extensive measurement of the quantity, distribution, and temperature of galactic dust. A new understanding of galactic structure will result, including spatial scales that are essentially unexplored in the infrared for our galaxy but which reproduce the spatial resolution of typical studies of external galaxies.

b) The measurement of diffuse emission from intergalactic material and/or galaxies and quasi-stellar objects. If observations of the diffuse radiation from clusters of galaxies are coordinated with the Infrared Astronomical Satellite (IRAS), so that selected clusters are well-observed at high and low spatial resolution, new information will be obtained on the intergalactic medium. Such observations will be particularly interesting when they pertain to clusters known to exhibit diffuse X-ray emission.

c) The measurement of the zodiacal dust emission. Calculations indicate that zodiacal dust emission is likely to produce the major contribution to the background over much of the far infrared if the Shuttle-induced H_2O column density can be held to less than 1×10^{12} mol/cm^2. The scanning and absolute flux measurement capability of this experiment makes it possible to measure the zodiacal emission and to distinguish it from other sources by its spectral and spatial distribution.

d) The measurement of a large number of discrete infrared sources which overlap with the results of IRAS. To distinguish between a true diffuse emission and the effect of one or more discrete sources in the beam, it is necessary to include spatial filtering. This provides measurements of the flux, spectral characteristics, positions, and sizes of discrete sources with a high sensitivity. Comparison of these results with those from IRAS will provide additional information on source spatial extent and source variability.

Technical and engineering objectives are primarily concerned with the measurement of the natural and spacecraft-induced infrared background, and the determination of suitable procedures and techniques for the in-space use of superfluid helium and cryogenic telescopes. In particular, these objectives are:

a) To make environmental measurements of H_2O, CO_2, and other infrared-active molecules, dust particles, and the effects of molecular deposition and cosmic rays; and to determine the effects of the induced Shuttle environment on the performance of cooled infrared telescopes.

b) To prove out the design of a cooled infrared telescope that can be applied to larger scale instruments (this includes, e.g., the design of the Sun shield and vacuum cover for a cooled telescope and protection of cooled optics against condensates.)

c) To demonstrate the performance of a large superfluid helium dewar system and measure certain properties of superfluid helium in space. Such aspects of cryogenic technology to be investigated include the storage and control in space of a large volume of superfluid helium, the long-term zero-g operation of a porous plug, and the transfer of refrigerant to a complex thermal load.

The instrumentation for the experiment is shown in Figure V-1 and a model of the experiment is shown in Figure V-2. It consists of a small telescope and infrared-detector array mounted inside a cryostat fed from a 250-liter superfluid helium dewar. The telescope consists of a cooled (8 K),

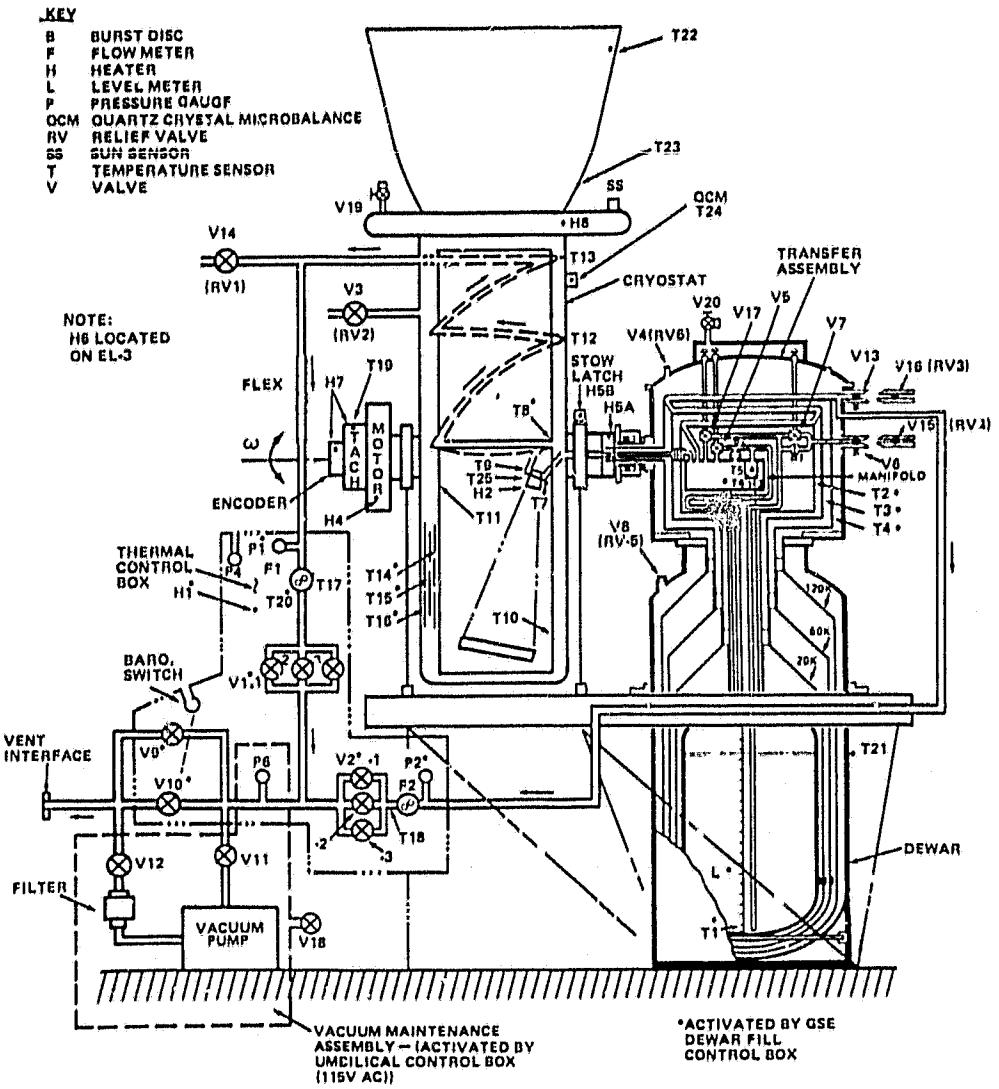

Figure V-1. Infrared telescope cryogenic instrumentation.

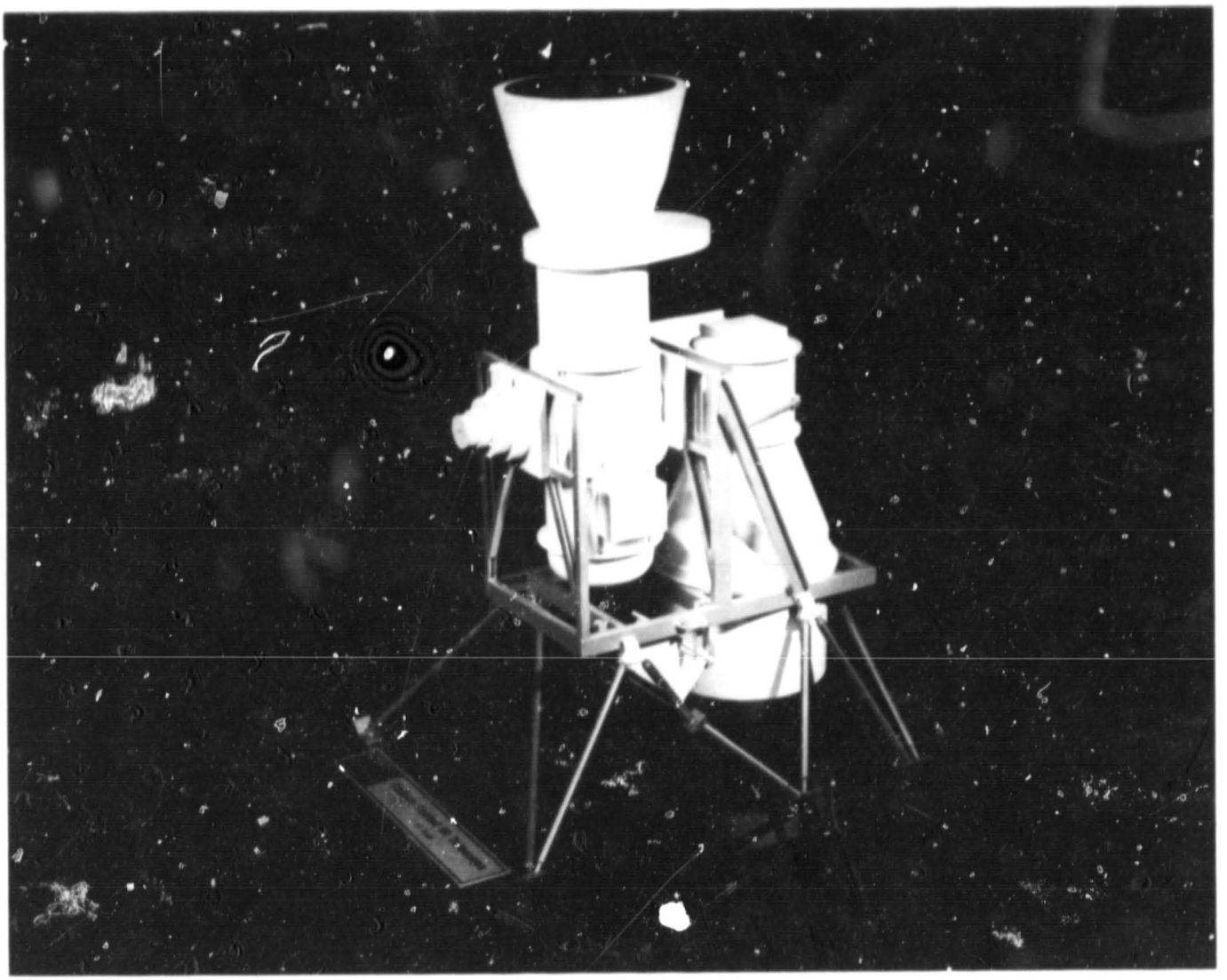

Figure V-2. Model of the small, helium-cooled infrared telescope experiment showing telescope and liquid-helium dewar.

highly baffled Herschelian optical system with an off-axis parabolic 15-cm diameter, f/4 primary mirror. The telescope is located within its own helium gas-cooled cryostat, which is a low-inertia articulated extension of the fixed, liquid-helium storage dewar. The telescope rotates in a plane about an axis parallel to the Shuttle x-axis. The scan plane rotates on the sky as the Shuttle pitches in its orbit around the Earth. Near the scan axis it has a drive motor at one end and the focal plane and cryogenic connection at the other end. It will scan at an angular speed of 6 degrees/sec and cover a 90-degree arc across the sky. The combined motions of the telescope and Orbiter permit each astronomical source to be detected at least twice on consecutive scans of the telescope and permit about 60 percent of the sky to be covered in one orbit, thus providing the redundancy necessary to discriminate among signals produced by particulates, man-made satellites, meteors, asteroids, variable stars, and ordinary stars.

The focal plane of the telescope contains ten detectors, nine of which cover the spectral region from 4 to 120 μ in four broad non-overlapping bands (4.5-8.5, 9-14, 18-30, and 70-120 μ) and one detector which has a narrow-band response at the H_2O band location (6-7 μ). All the infrared detectors are masked with a single bar to modulate the signal of compact sources as they cross the array.

The detectors in each channel have been arranged to cover a full 3 degrees perpendicular to the scan direction. The tenth detector is a star sensor masked with an N-slit, sensitive in the 2-3 μ band. A moveable cold shuttle has also been included to provide an absolute "zero" flux reference for each of the detector bands. The need to maintain the focal plane array at a temperature of approximately 3 K and the mirror of the infrared telescope at 8 K for an extended period of time requires the use of a stored liquid helium cooling system. The cryogenic system for this experiment is composed of a liquid-helium dewar containing liquid-helium II at a temperature of approximately 1.5 K, a transfer assembly with liquid-vapor separator, a vapor-cooled telescope cryostat, and a cryostat vacuum cover.

The cryogenic system must deliver adequate refrigeration to the infrared telescope cryostat in the form of cold vent gas circulating in the vapor-cooled shields. The cold gas evolves at a temperature of approximately 1.5 K from a porous plug which is fed from the supply dewar by a liquid supply tube within the transfer assembly. The cold gas is then divided into two vent line flows. One gas flow is used to cool the cryostat while the other returns to vapor-cool the radiation shields in the dewar. The helium supply dewar has a capacity of 250 liters. Physical characteristics of the experiment are listed in Table V-1.

TABLE V-1. PHYSICAL CHARACTERISTICS

Dimensions: 212 X 108 X 340 cm (Pallet)
Total Mass: 770 kg
Average Power: 100 W at 28 Vdc
Total Energy: 15 kWh
Data: 614 kbps (continuous)

VI. ELEMENTAL COMPOSITION AND ENERGY SPECTRA OF COSMIC RAY NUCLEI BETWEEN 50 GeV PER NUCLEON AND SEVERAL TeV PER NUCLEON
(2SL-06)

Peter Meyer and Dietrich Müller
University of Chicago

The abundance distributions of elements and isotopes in the cosmic radiation are a key for understanding the origin of the energetic particles. The past two decades have brought considerable advances in this field. Nevertheless, important aspects have as yet remained unexplored. Among these is the elemental composition at energies beyond 100 GeV/nucleon. There are several reasons why it is of great interest to study the composition of cosmic rays at high energies. It was found, with balloon-borne experiments performed in the investigators' laboratory and by others, that between a few GeV/n and 100 GeV/n, the cosmic ray composition undergoes drastic changes. The major effect involves the abundance of those nuclei which predominantly originate in nuclear collisions with the interstellar gas as compared to the species that originate in the cosmic ray sources. This work has clearly shown that at high energies, the cosmic rays traverse less interstellar matter. This effect could have several causes. Either high-energy particles have a greater probability to escape from the galaxy and hence a shorter containment time than low-energy particles; or the energetic particles, if contained for the same length of time, spend a larger fraction of their life in regions of the galaxy which contain much less interstellar gas. Finally, the effect could also be caused by one or several cosmic ray sources which emit predominantly high-energy particles and are located in the vicinity of the solar system. This appears to be the least likely possibility; however, the alternatives have been discussed in the literature. No unique interpretation has so far been found because of the limited statistical accuracy of the existing data and the limited range of measured energies. It is clear that these questions are directly tied to the problem of the particle transport in the galaxy and the distribution of matter and fields. For instance, this involves the question of the role of a galactic halo for particle confinement, which was proposed by Ginzburg many years ago.

Another important question is whether the relative abundances of different source nuclei change with energy. While this effect could not yet reliably be established in balloon experiments, its implications are extremely interesting. Direct evidence for the contribution of different sources to the flux of cosmic rays is expected to come from variations of the relative abundance of source nuclei with energy. Several airshower experiments have claimed that the source composition changes drastically at high energy, but these experiments cannot provide any detail. Statistical accuracy, extended energy coverage, and unique identification of each particle are needed to provide information about the nature of the source of energetic cosmic rays and about the processes involved in their acceleration.

The major limitations in past experiments were: limited size of the instruments and limited exposure time to the particle flux. The University of Chicago experiment on Spacelab 2 overcomes these limitations and explores the cosmic ray composition to energies more than 10 times those presently reached. The experiment makes full use of the unique capabilities of the Spacelab carried on the STS, by exposing an instrument of large volume and considerable mass for an extended period of time, and uninfluenced by any overlying atmosphere. The experiment can provide sufficiently large exposure factors (geometry X time) and excellent elemental resolution to allow abundance determination with good statistical accuracy to several 1000 GeV/nucleon, where, because of the shape of the cosmic ray spectrum, the flux is very small. In fact, the experiment will approach the important region of ultra-high energies where thus far only indirect measurements through air shower observations

were possible whose interpretation led to controversial results on the composition of the primary particles. An important reason that makes this experiment feasible stems from the fact that novel techniques for energy measurements have recently become available. Two such techniques have been extensively studied and have been used successfully for the first time in balloon experiments in the investigators' laboratory. They are: (a) gas Cerenkov counters and (b) transition radiation detectors. Both possess a unique feature absent in most other instruments for very energetic particles: they require detectors of low density and hence relatively light weight, thus permitting construction of the needed very large area instrument within the weight constraints that even Spacelab imposes.

The detector elements are contained in a cylindrical pressurized shell with hemispherical top and bottom covers (diameter 2.8 m, maximum height 3.7 m) as shown in Figure VI-1. All detector elements will comprise areas of 2 X 2 m. The large dimensions of the instrument yield a geometric factor of approximately 5 m^2 ster for the transition radiation detector and approximately 1 m^2 ster for the Cerenkov counter telescope. Physical characteristics of the experiment are listed in Table VI-1.

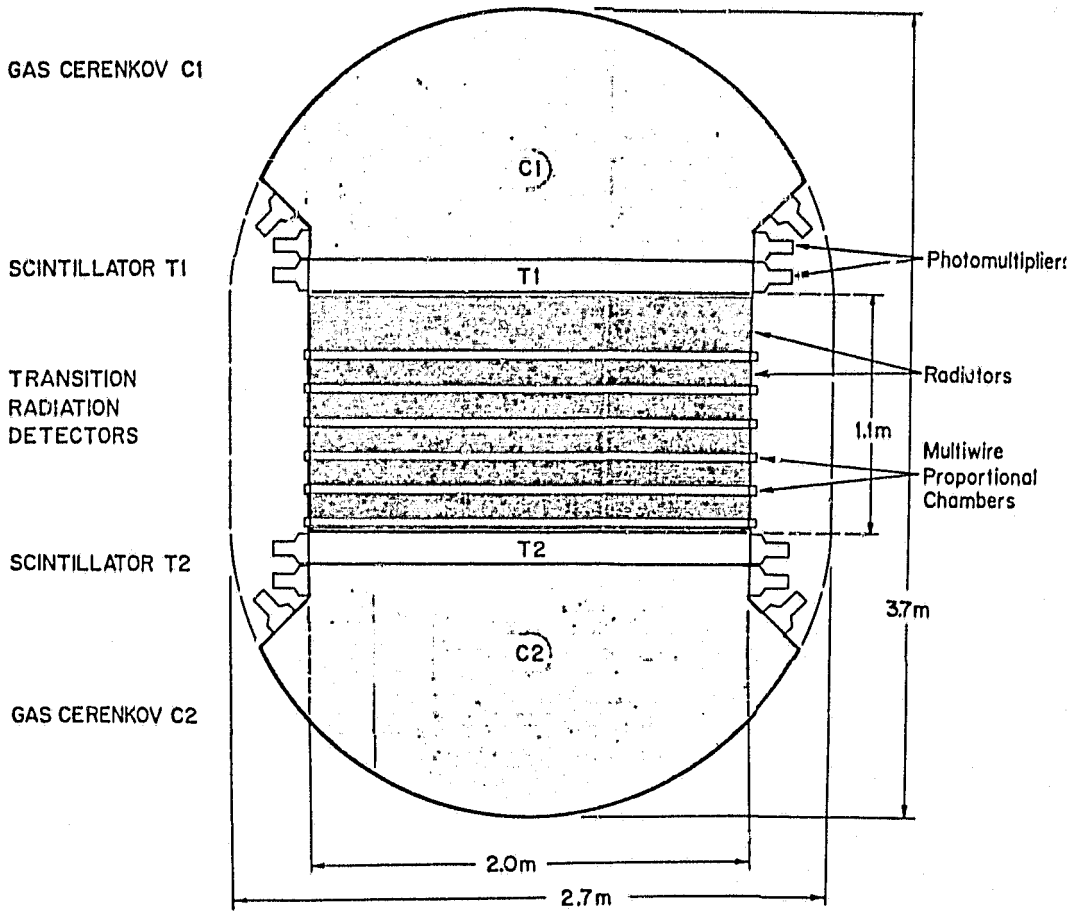

Figure VI-1. Cosmic ray experiment.

The instrument is designed to measure the charge composition in the range Z = 3 (Lithium) to Z = 28 (Nickel) and the energy spectra from approximately 50 GeV/n to at least 2000 GeV/n. Figure VI-1 shows a schematic cross section of the counter telescope. The charge of the incident particles is determined by their energy loss in two scintillation counters, T1 and T2. Energies between about 50 and 150 GeV/n are measured by determining pulse heights in the two gas Cerenkov counters,

TABLE VI-1. PHYSICAL CHARACTERISTICS

Dimensions:	
Detector Assembly:	270 X 270 X 370 cm
Total Mass:	1968 kg
Average Power:	331 W at 28 Vdc
Total Energy:	47 kWh
Data:	102 kbps

C1 and C2, which are filled with a mixture of Ne and CO_2. (This gas fills the entire pressure shell enclosing the detector.) Energies between about 400 and 4000 GeV/n are measured with a transition radiation detector. This detector consists of a stack of radiators alternating with multiwire proportional chambers. The radiators are made of polyethylene fibers, a novel approach, developed and used for the first time in the University of Chicago laboratory and for this experiment. Extensive tests made at the Fermi National Accelerator laboratory and the University of Bonn Synchrotron have verified that the fiber radiators are equivalent to, or even better than, radiators made of foils. The multiwire chambers are filled with a gas mixture of Xe, He, and CH_4 to optimize the relative signal strength from the transition radiation X-rays and from the ionization loss of the penetrating particles. The multiwire chambers simultaneously serve as a hodoscope which determines the trajectory of each particle. This permits determination of the angle of incidence and point of traversal for each counter, thereby allowing corrections that will optimize charge resolution. Information from the various sensors will be collected by an electronics package and formatted for ground transmission.

Figures VI-2 and VI-3 show the instrument in two stages of assembly. Figure VI-2 shows the assembly of two layers of radiators between, and on top of, two multiwire proportional chambers. Figure VI-3 shows the integration of the upper photomultiplier assemblies for the Cerenkov and scintillation counters with two layers of the transition and radiation module.

Figure VI-2. Assembly of two layers of radiators between, and on top of, two multiwire proportional chambers.

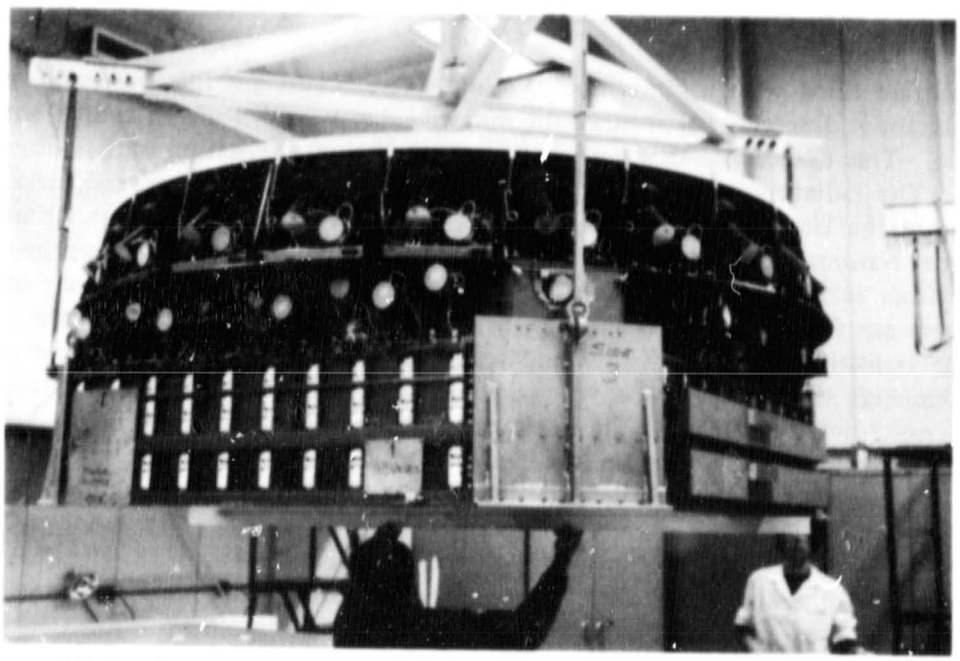

Figure VI-3. Integration of upper photomultiplier assemblies of Cerenkov and scintillation counters with two layers of the transition and radiation module.

VII. HARD X-RAY IMAGING OF CLUSTERS OF GALAXIES AND OTHER EXTENDED X-RAY SOURCES
(2SL-07)

Peter Willmore
University of Birmingham, United Kingdom

One of the unexpected results to come from early work on X-ray astronomy was that certain clusters of galaxies are extended sources of X-rays. In fact, the majority of X-ray sources identified at high galactic latitudes are clusters of galaxies. A number of different theories and models to explain the emission have been proposed. For example, one possibility is that the emission is thermal bremsstrahlung from a hot intergalactic gas. Using this model, X-ray measurements would provide a means of observing an otherwise invisible component of the clusters and of studying its temperature and mass distribution. The total mass of such a gas might actually exceed the observable mass within the galaxies themselves. Such a cloud might well represent the matter from which the galaxies were formed; alternatively, it may be continuously streaming from active galaxies. In either case, it would be of considerable interest. Among other things, an understanding of the properties of the intergalactic gas would be an important contribution to the theory of radio sources.

In another main class of models the X-ray emission is assumed to result from inverse Compton interactions between high-energy electrons and the photons of the 2.7 K microwave background. On the basis of these models the synchrotron radio emission caused by the interaction of the high-energy electrons with the intergalactic magnetic fields would be expected to correlate strongly with the X-ray emission. The intensities should be directly related, and the spectra should have the same form since they depend in the same way on the electron energy distribution. Thus, the X-ray observations would allow the spectrum and distribution of GeV electrons in the clusters to be directly deduced; and, in combination with radio observations, this would provide a measurement of the intergalactic magnetic fields. Such direct evidence might well make an impact on the problems of the origin and containment of the high-energy electrons in nonthermal radio sources.

Observations of the X-ray spectra, in principle, allow a choice between emission mechanisms. However, only the spectra of the three brightest cluster sources, those in Perseus, Virgo, and Coma, and more recently that of the Centaurus clusters have been studied in detail. The form of the spectra and the indications of iron line emission strongly favor thermal models, but the results do not allow any definite conclusions to be drawn. As yet, only for the Perseus cluster is anything known of the spectra of the separate parts as distinct from the overall integrated spectrum. Different spectra from the different parts of the source have been reported, which may account for the difficulty in applying simple models or theories to overall spectra.

At present, X-ray flux is believed to have been observed from approximately 55 clusters of galaxies, although in some cases this simply means that an X-ray source is known to exist within an error box of perhaps one square degree containing the center of a catalogued cluster. In six cases the X-ray source is known to be extended. Only for the three strongest sources are any useful spectral information and any detail of the spatial structure beyond a single size parameter available. Yet it is already clear that there are differences — e.g., in X-ray luminosity and in spectral steepness — between the sources, and data on one or a few do not necessarily allow deductions to be made about the whole class. Clearly, better observations are necessary.

This experiment comprises a double X-ray telescope, shown schematically in Figures VII-1 and VII-2, which uses a novel but proven technique to produce X-ray images of small regions of the sky at higher X-ray energies than is possible using conventional methods. It will be used primarily to examine the emission from clusters of galaxies to study the mechanisms involved in their emission and the possible presence of an intergalactic gas. It will investigate the spatial and spectral distribution of X-ray flux from these clusters in the energy range 2 to 20 keV. The experiment will also be used on other X-ray sources such as those occurring at the center of our galaxy. The sources of interest are extremely weak, and to accumulate sufficient observing time on a reasonable number of targets the experiment will be equipped with its own pointing system and microprocessor controller, thus enabling it to operate while other experiments have prime observing time. The hardware for the frame of the telescope is shown in Figure VII-3.

The telescope system uses a coded binary mask and a position-sensitive detector, and is capable of producing an X-ray map of a given region of the sky. The telescope system utilized for the observations uses a variation of the Dicke random pinhole mask technique. A mask is used in which a pseudorandom pattern of holes replaces the random pattern. The mask produces a shadowgram on the position-sensitive detector when illuminated by radiation from the object and an image of the object is reconstructed by deconvolving the mask pattern from the shadowgram.

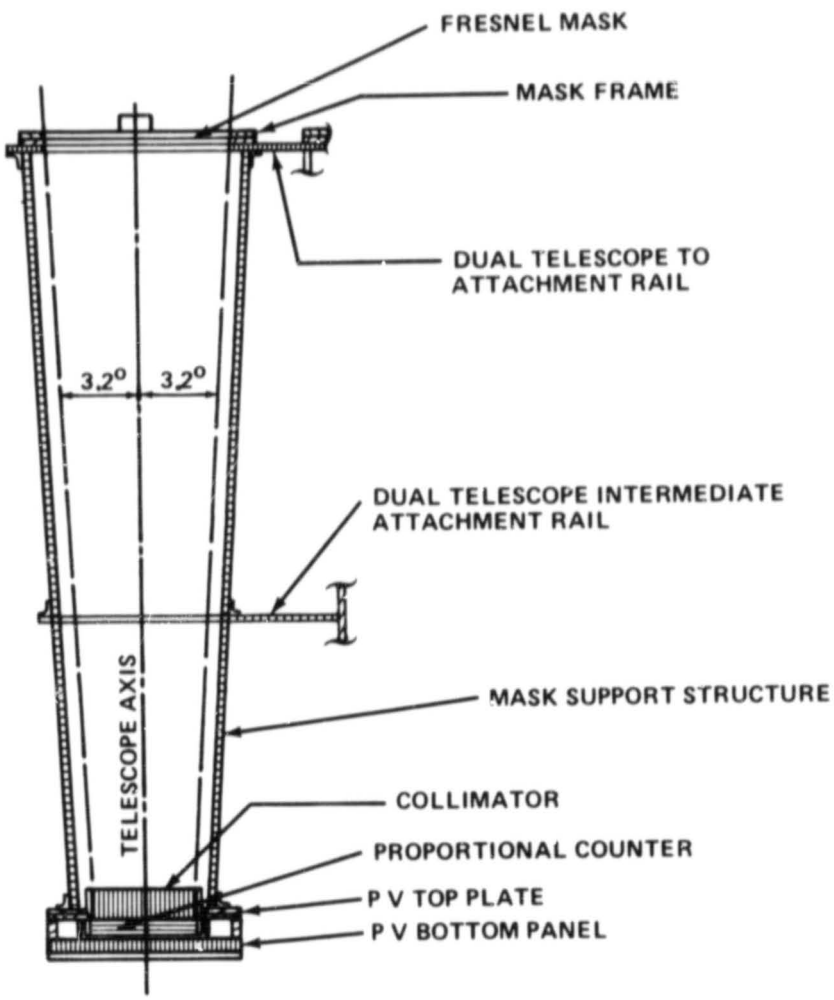

Figure VII-1. Sectional arrangement of X-ray telescope.

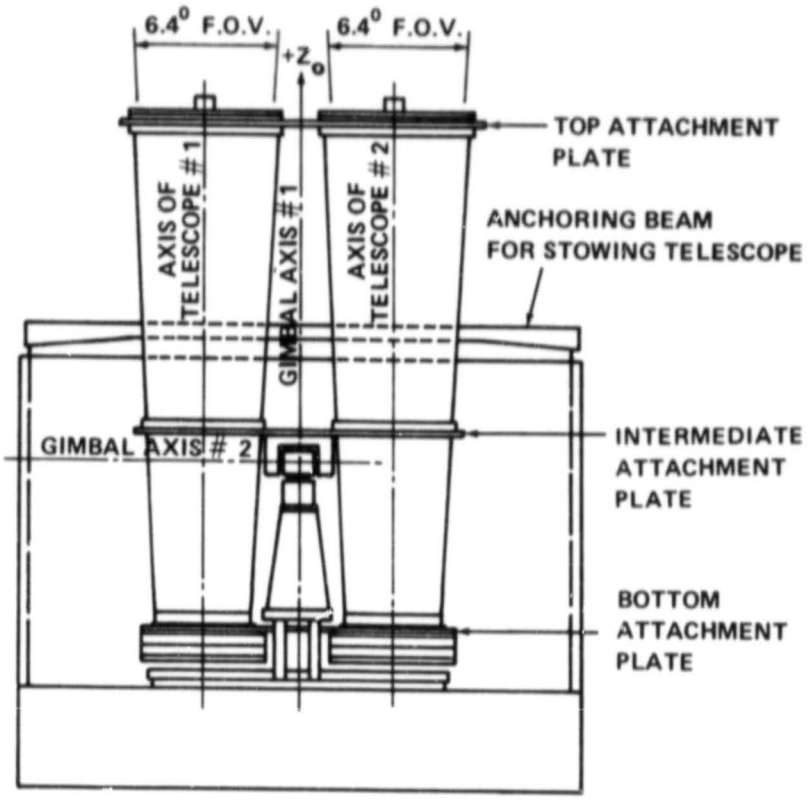

Figure VII-2. Side view of the X-ray telescope.

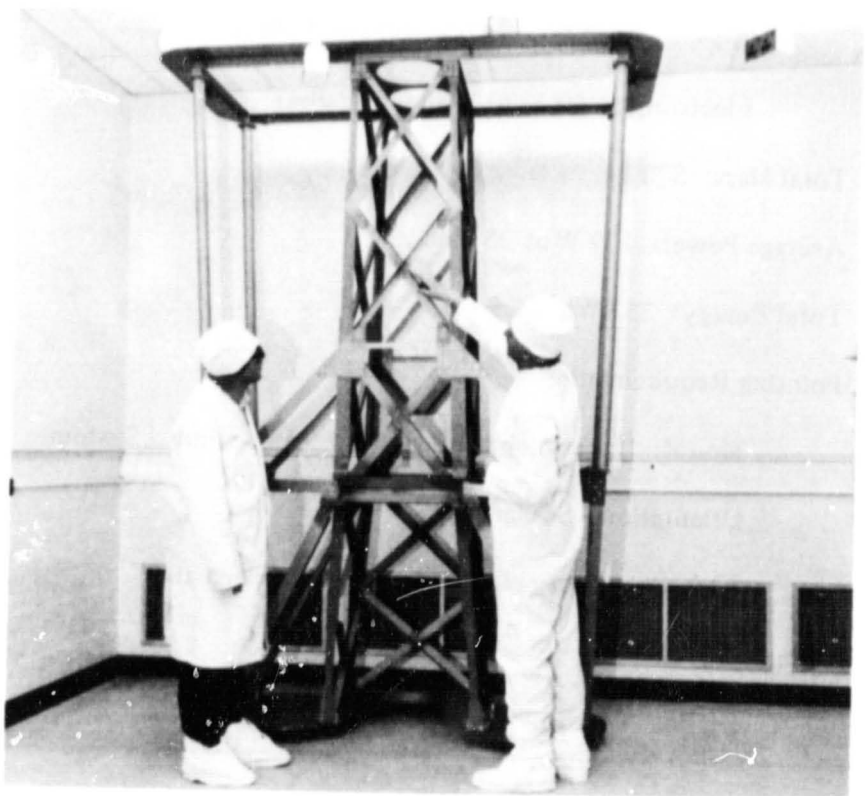

Figure VII-3. Frame of the double X-ray telescope assembly.

The optimum choice of telescope resolution depends on the signal-to-noise ratio and the size and form of the sources to be studied. Because the surface brightness of a source determines the signal in an image element of a particular size and because the surface brightnesses of the clusters vary considerably, two telescopes are utilized with different values of resolution: a coarse resolution to detect faint sources and extended regions of stronger sources, and a fine resolution system capable of resolving fine details in more intense regions. The values of these resolutions are 3 X 3 arc min and 12 X 12 arc min. These figures refer to the full width half maximum (FWHM) of the response and do not necessarily imply the limits to the fineness of the detail which can be deduced.

Multiwire, position-sensitive proportional counters will be used as detectors. They will be able to determine the position of arrival and the energy of each photon. Anti-coincidence techniques will be utilized to reject cosmic-ray events.

Other features of the telescope system include a motorized gimbal system which is capable of pointing the telescope system to within 0.5 degree of any required orientation with respect to the Shuttle; a microprocessor system to accept the nominal vehicle attitude from the Shuttle data system, to select an accessible target from a preprogrammed list, and to drive the telescopes to the correct orientation; a gyro package to determine the actual pointing direction; star sensors to aid in the determination of absolute directions to better than 1 arc min; and star field cameras for analysis of long-term drift motion. The physical characteristics of the experiment are listed in Table VII-1.

TABLE VII-1. PHYSICAL CHARACTERISTICS

Dimensions:
Telescopes: 206 X 335 X 100 cm (Pallet)
Electronics: 60 X 30 X 30 cm (Pallet)
Total Mass: 570 kg
Average Power: 179 W at 28 Vdc
Total Energy: 25 kWh
Pointing Requirements:
Mount: Experiment-Provided Two-Axis Gimbal System
Orientation: Stellar
Accuracy: 3 deg maximum (0.5 deg design aim)
Data:
Digital: 64 kbps

VIII. A SOLAR MAGNETIC AND VELOCITY FIELD MEASUREMENT SYSTEM (2SL-08)

Alan Title
Lockheed Solar Observatory

Magnetic fields play a crucial role in determining the structure and dynamics of the solar atmosphere, from the deepest visible levels of the photosphere, upward through the chromosphere and corona, and out into the interplanetary medium. During the past 20 years, astronomers have accumulated a great mass of information on large-scale magnetic structures using photographic and photoelectric magnetographs. However, magnetograms and velocitygrams of small features have proven very difficult to interpret, primarily because of blurring and distortion of images by the Earth's atmosphere. Despite the presence of several superb ground-based ilities, little further advance can be expected in defining the details of the small-scale structures, du the inherent limits imposed by atmospheric seeing. However, with spaceborne observations, the image degradation produced by the atmosphere can be avoided and diffraction-limited images free from geometric distortion can be obtained. This advantage may be used to observe the strength, geometry, and evolution of the elemental magnetic field points in the solar atmosphere and to determine the interaction of these magnetic elements with the solar velocity fields.

The Solar Magnetic and Velocity Field Measurement System will use this advantage to achieve a spatial resolution and temporal coverage impossible to attain from observatories on the ground. The objectives of the experiment are: (1) to measure magnetic and velocity fields in the solar atmosphere with high spatial resolution and to deduce the small-scale structure and evolution of these fields on the 10- to 20-min time scale of solar granulation; (2) to follow the evolution of solar magnetic structures over periods of several days to determine how the magnetic elements couple to the supergranule velocity patterns and by what mechanisms field diffusion and disappearance occur; (3) to study with high temporal and spatial resolution the magnetic field changes associated with transient events, such as flares, and to isolate and follow the birth of sunspots, pores, and ephemeral regions; and (4) to provide a test of the pointing accuracy and stability of the Instrument Pointing System (IPS) to subarc second accuracy.

To achieve these objectives, the experiment consists of a Solar Optical Universal Polarimeter (SOUP) mounted on the IPS. For optics, the polarimeter utilizes a 30-cm Cassegrain telescope designed for diffraction-limited performance in the wavelength region 4800 to 7000 Å. An effective gimbal system for the entire package in conjunction with a solar limb tracker allows the observation of any point on the solar disk when the IPS is directed within several degrees of the Sun. Two independent focal plane systems are used for the observations. The first is a white-light system which records granulation and pointing data onto film for video display at the Payload Specialist station. The second, a tunable filter system, consists of a tunable birefringent filter with a selectable bandpass of 30 mÅ or 70 mÅ, and associated blocking and polarizing filters to produce monochromatic images in a known state of circular or linear polarization. The wavelength of the resulting image is selectable to within ±4 Å of any of nine predesignated spectral lines. The resulting filtergrams will be recorded on SO-115 film and with a diode array camera. The diode array output is fed into the video processor, which is capable not only of image storage but also of directly adding, subtracting, multiplying, or dividing images into any or all of its six internal image memories. In this manner, magnetograms and velocitygrams will be made in real time. A schematic of the instrumentation is portrayed in Figure VIII-1, while the experiment canister is shown in Figure VIII-2. The physical characteristics of the experiment are listed in Table VIII-1.

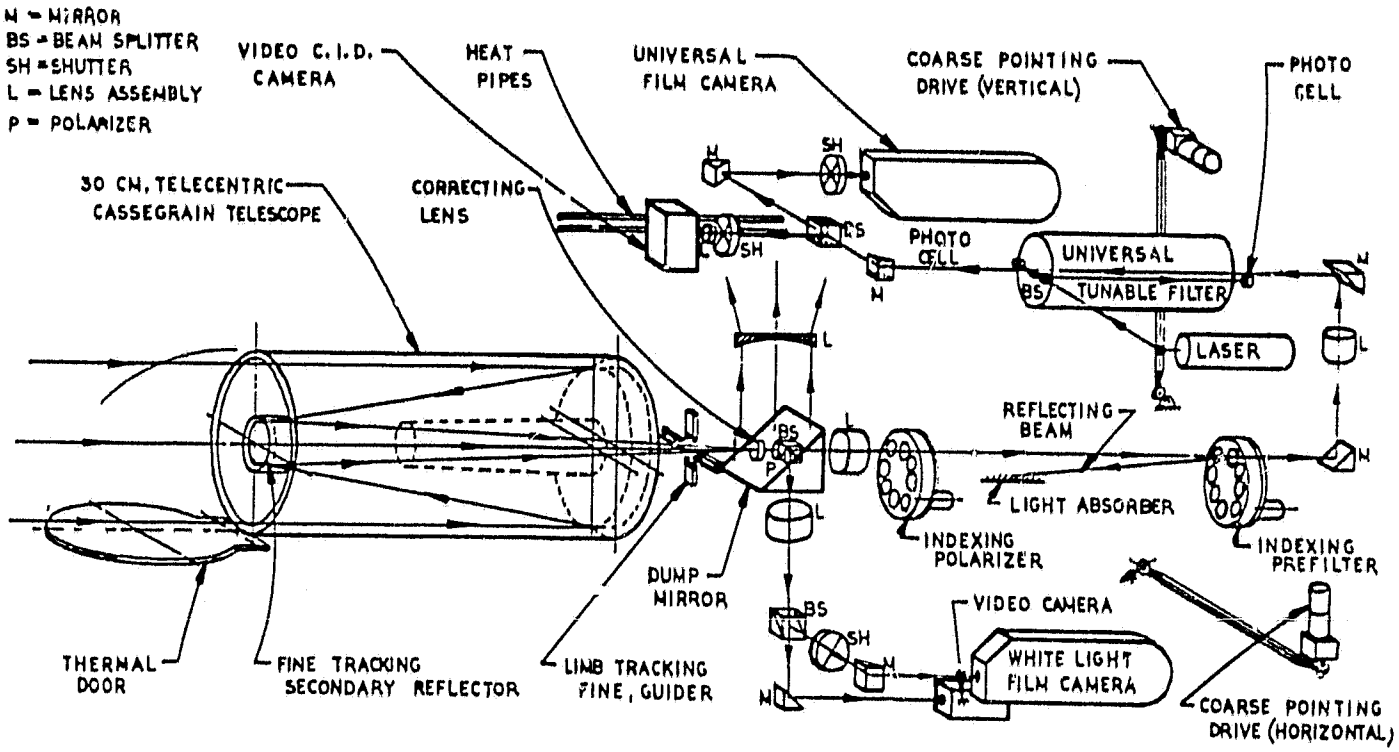

Figure VIII-1. The optical/mechanical schematic of the Solar Optical Universal Polarimeter.

TABLE VIII-1. PHYSICAL CHARACTERISTICS

Dimension:

Telescope and Focal Plane Structure: 40 X 40 X 205 cm (Pallet – IPS)
Processor: 56 X 48 X 36 cm (Pallet)

Total Mass: 248 kg

Average Power: 150 W at 28 Vdc

Total Energy: 22 kWh

Pointing Requirements:

Mount: IPS
Orientation: Solar
Accuracy: 2 arc sec
Stability: ±15 arc sec

Data:

Digital: 1.4 Mbps
Film: Type SO-115
TV: 4.2 MHz

In one operating mode, the SOUP will produce spectroheliograms, Dopplergrams, and conventional magnetograms (maps of the line-of-sight component) within a short time scale. For studies of rapid oscillations and transients, magnetic lines at two heights and H_α can be covered in less than 15 sec. A second operating mode is to take multi-frame wavelength scans through a line profile, with either pairs of orthogonal polarizations or quartets (Stokes parameters) taken at each wavelength step. After the mission, these images will be merged to provide polarized line profiles at each point for further analysis.

After data reduction, the photoelectric magnetograms, velocitygrams, and white-light movies will provide quantitative maps of photospheric brightness, magnetic flux, and line-of-sight velocity. The scientific results from the study of these maps will include: (1) the sizes, strengths, and polarities of magnetic regions in the photosphere and some information on their vertical structure; (2) the motion of flux tubes under the influence of granular and supergranular velocity fields, including the evolution of the supergranular network; (3) the lifetimes of magnetic regions and the mechansim of their disappearance or annihilation; (4) the relation of chromospheric structures (spicules, rosettes, dark mottle, etc.) to the underlying photospheric magnetic structures; (5) time series analysis leading to frequencies and phase relations of magnetic and velocity oscillations; (6) the nature of pore and sunspot formation and decay; (7) information on the range of field strengths present in the photosphere outside the sunspots; and (8) the motion and evolution of the weak bipolar fields found in the interiors of supergranular cells. If a flare is observed, the transients in magnetic fields, velocities, and brightness before and during the flare will be estimated.

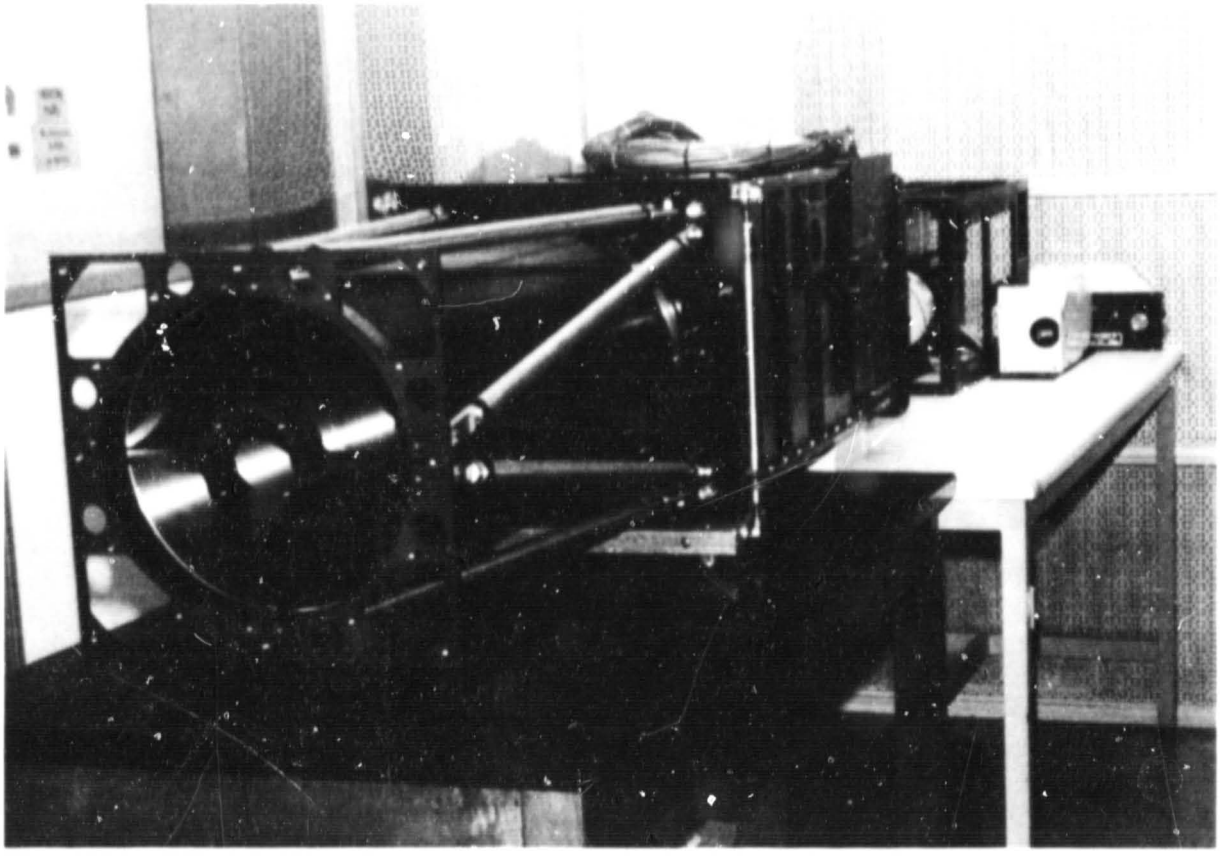

Figure VIII-2. Solar Optical Universal Polarimeter (SOUP) hardware.

Analysis of the polarized line profiles will yield maps of continuum and line center brightness, equivalent width, Doppler velocity, magnetic field strength, and magnetic flux. In addition, analysis of sunspot profiles will give their components of the magnetic field vector. Results of the study of these maps will include: (1) the distribution of magnetic field strengths in the photosphere as a function of area covered by the magnetic regions; (2) estimates of the magnetic energy density and stress tensor to test theories of field concentration, confinement, motion, and diffusion; (3) estimates of the energy transport by MHD wave propagation to test theories of the energy balance of sunspots, the chromosphere, and the corona; (4) the frequency of occurrence of strong transverse field components, in and outside of sunspots; (4) changes in the vector magnetic field and its energy content during a flare, should one occur during the observations; (6) quantitative field-line configurations in sunspots, to test theories of spot formation and stability; and (7) evaluation of the accuracy of the force-free approximation in vector field calculations, the only known method for computing fields throughout the chromosphere and corona from magnetograph observations. Finally, the data base of high-resolution line profiles will be available to theoreticians for sophisticated modeling of the physics of magnetic structures in the solar atmosphere.

IX. CORONAL HELIUM ABUNDANCE SPACELAB EXPERIMENT (CHASE) (2SL-09)

Alan H. Gabriel
Rutherford and Appleton Laboratory, United Kingdom

and

J. Leonard Culhane
University College, United Kingdom

The CHASE experiment is aimed at deriving an accurate measure of the solar helium abundance and, at the same time, performing useful studies of the XUV emission from coronal and active regions. Helium constitutes approximately 10 percent of all atoms in the universe. However, its abundance in the Sun and other astronomical objects is only approximately known. The element is important in relation to a number of physical processes in the Sun, including nuclear processes in the core, opacities in the photosphere, and radiative energy transport in the chromosphere.

Current cosmological theories indicate that most of the helium in the universe must be of primeval origin, with only a negligible fraction resulting from stellar nucleosynthesis. In this case, one expects the relative helium abundance to be uniform everywhere. Since helium provides a major contribution to opacities and radiative loss effects, its abundance is important to all aspects of stellar evolution and stellar modeling. Furthermore, an accurate value of this abundance is of vital importance for theories of the origin of the universe, since it must be closely related to conditions during the original big bang. Clearly, the determination of an accurate value for the Sun, the most studied of all stars, would be of considerable value.

Nevertheless, an accurate derivation of the solar helium abundance has proved difficult to perform. Because of their high excitation potential, He I lines are formed in the Sun at high temperatures in the chromosphere and in regions where the situation is complicated by inhomogeneities associated with the chromosphere network and spicules. Thus, normal methods for determining abundances from photospheric absorption lines cannot be applied. However, the CHASE experiment will observe the hydrogen (1216 Å) and ionized helium (304 Å) resonance lines formed by photo excitation of the coronal material. Here, the hydrogen and helium line emission is due mainly to the resonance scattering of the intense chromospheric emissions at these wavelengths. The experiment will look at the light source (disc) and the scattering region (corona above the limb); and because the two principal lines are common in both cases, the results are independent of instrument intensity calibration. Second-order effects in the calculation are due to electron density and temperature which can be adequately measured by line ratio methods. It is anticipated that the relative helium abundance will be established to better than 5 percent, and in a manner which is independent of most of the assumptions regarding atmospheric models.

Several experiments, for example, the Harvard experiments on OSO 4 and 6, have carried out solar XUV observations; however, relatively few have extended their coverage into the grazing incidence region below 300 Å. Clearly then, there is some advantage in enhancing the instrument specification to provide a facility capable of more general solar XUV studies. The CHASE experiment (shown schematically in Fig. IX-1) utilizes a 1-m grazing-incidence spectrometer with a 1200 lines/mm concave grating. The image of the Sun is focused onto the entrance slit plane by means of a 28-cm focal length grazing incidence telescope of Wolter type I section design.

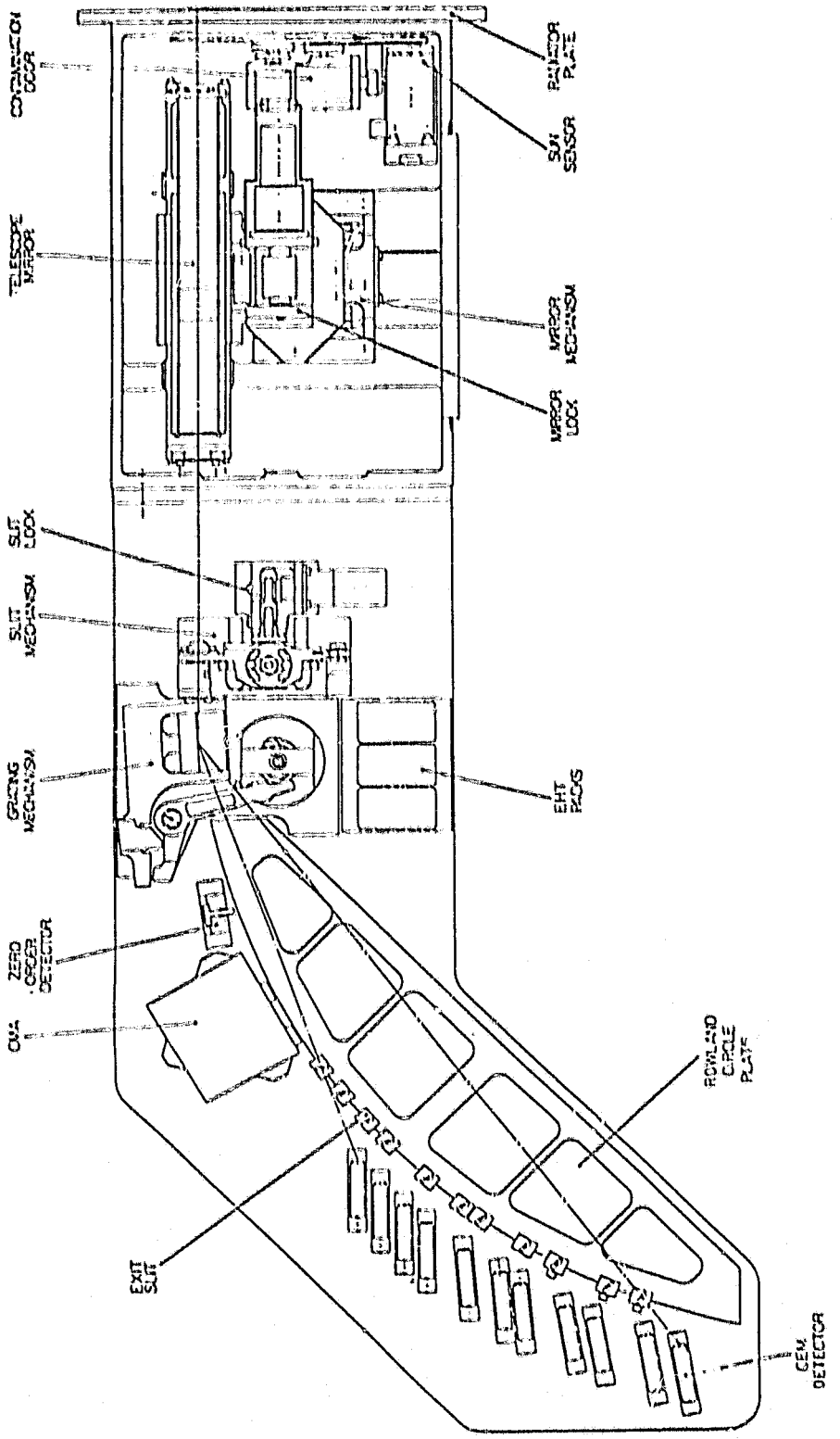

Figure IX-1. Schematic representation of the CHASE experiment.

Eleven channel electron multipliers are placed behind individual exit slits that are positioned on the Rowland Circle to accept preselected wavelengths. Two such detectors will monitor the hydrogen Lyman α (1216 Å) and He II (304 Å) lines, each directly associated with the He/H abundance measurement. The other detectors monitoring ionized lines of Fe, S, C, and O will cover associated parameters such as the temperature and density of the solar atmosphere. In addition to the single-channel multipliers, a channel multiplier array will also be positioned on the Rowland Circle. In operation, this is similar to the detector array inside a TV camera and will allow several emission lines to be monitored simultaneously.

The scientific specifications of the overall instrument can be summarized as follows: (1) an adequate sensitivity and dynamic range to record emission lines on the disc and above the limb, (2) a pointing capability to better than 5 arc sec, (3) a spatial resolution of $\sim$ 15 arc sec, (4) a spectral resolution $\lesssim$ 0.5 Å, and (5) an ability to provide one- and two-dimensional scans.

The experiment is mounted on the ESA Instrument Pointing System (IPS) which is capable of providing sufficient pointing control. However, with three other solar experiments on the IPS, some independent pointing is desirable. This requirement is fulfilled by the construction of scan platforms for both the mirror and the slit. Both motions are mutually perpendicular and allow two-dimensional raster scans to be performed. The total offsets involved are ±20 arc min for the mirror and ±15 arc min for the slit, both having a step resolution of 10 arc sec. The slit mechanism fulfills the dual purpose of pointing control and slit size selection.

It is necessary in the helium abundance experiment to measure the intensity on either side of the emission line, contributions to which could arise from a true solar continuum or from scattered light. To achieve this, a small wavelength scan is effected by rocking the grating. In this way, the wavelength range is increased at moderate cost to resolution, with the additional bonus of access to more emission lines. Total scan is ±400 arc sec with a 5 arc sec step, this range being equivalent to $\sim$ ±10 Å at hydrogen Lyman α.

A further refinement to the instrument is the provision of a sun sensor. This will be aligned to the instrument's optical axis prior to flight and will serve to monitor any misalignments occurring between the instrument and the IPS pointing direction. A static misalignment could easily occur at launch, but more serious would be variable offsets resulting from thermal drifts occurring on-orbit.

A final mechanism takes the form of a closeout shutter which will protect the mirror from contamination during launch and experiment shut-down periods.

The operational flexibility of the instrument is maximized by the incorporation of a dedicated experiment microprocessor. Pre-programmed sequences initiated from either the crew station or the ground control center will be used for mechanism control and data processing prior to transmission. During the mission, the sequences may be modified or, if necessary, replaced.

The physical characteristics of the instrument are listed on Table IX-1. A view of the engineering mockup is shown in Figure IX-2.

TABLE IX-1. PHYSICAL CHARACTERISTICS

Dimensions:

CHASE Instrument: 56 X 44 X 115 cm (Pallet-IPS)

Microprocessor: 37 X 36 X 30 cm (Pallet-IPS)

Power Supply: 35 X 33 X 30 cm (Pallet-IPS)

Total Mass: 114 kg

Average Power: 72 W at 28 Vdc

Total Energy: 11.7 kWh

Pointing Requirements:

Mount: IPS

Orientation: Solar

Accuracy: 15 arc sec

Stability: 5 arc sec

Data: 8.2 kbps

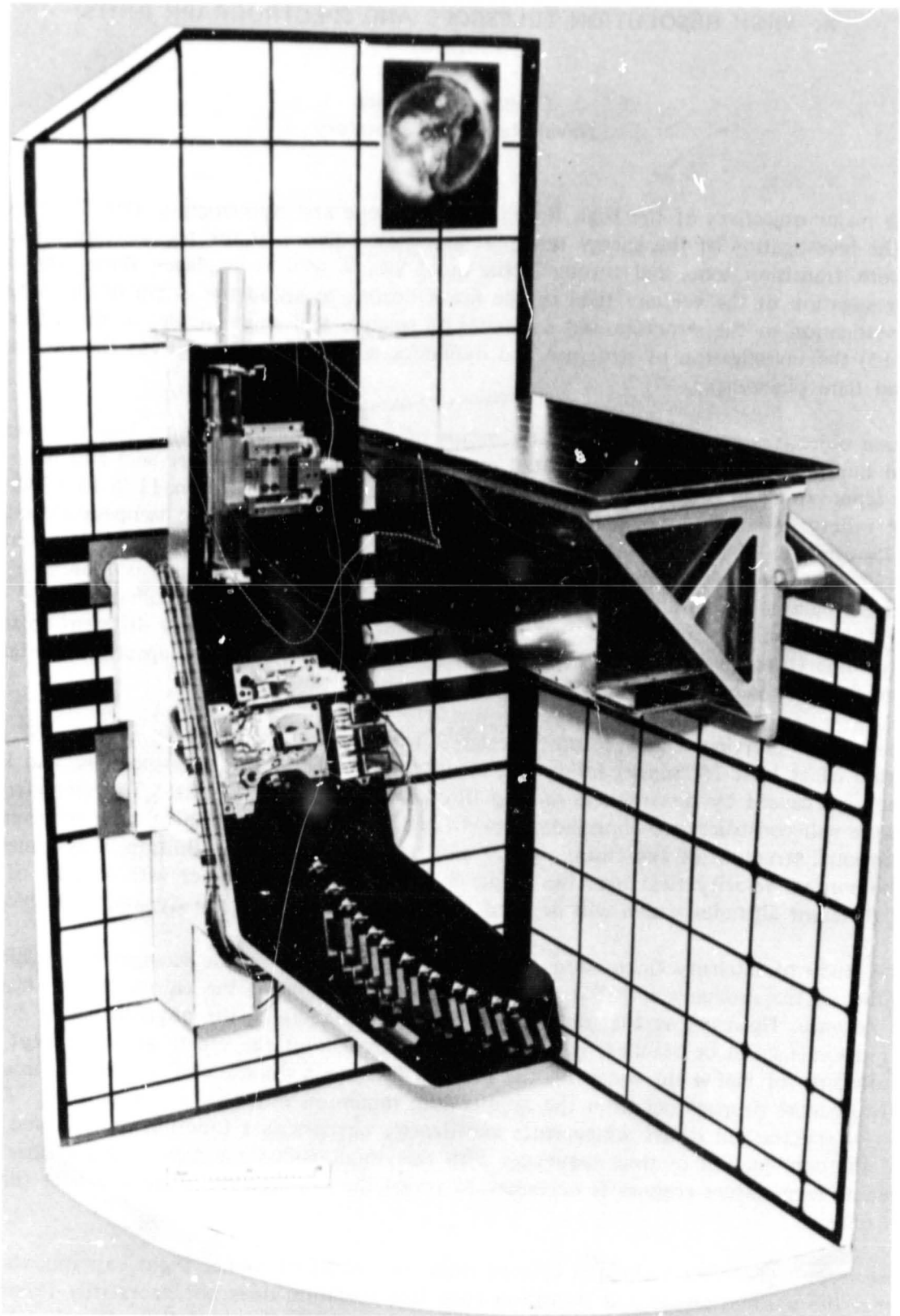

Figure IX-2. Engineering mockup of CHASE. The boxes to the side of the instrument house the microprocessor and analogue circuitry.

X. HIGH RESOLUTION TELESCOPE AND SPECTROGRAPH (HRTS) (2SL-10)

Guenter Brueckner
Naval Research Laboratory

The major objectives of the High Resolution Telescope and Spectrograph (HRTS) experiment are: (1) the investigation of the energy transport and mass balance of the temperature minimum, chromosphere, transition zone, and corona in the quiet Sun as well as in plages, flares, and sunspots; (2) the investigation of the velocity field of the lower corona to study the origin of the solar wind; (3) the investigation of the structure and dynamics of spicules and superspicules in the ultraviolet spectrum; (4) the investigation of structure and dynamics of prominences; and (5) the investigation of preflare and flare phenomena.

These objectives are to be achieved by means of intensity measurements, Doppler measurements, and line profile analysis of high spatial resolution (approximately 1 arc sec) and high spectral resolution (approximately 0.05 Å) ultraviolet spectra in the wavelength region 1176 to 1700 Å, covering a wide variety of continua and emission lines which originate in different temperature regimes of the solar atmosphere. A stigmatic spectrograph to be used for this investigation provides simultaneous coverage of continua and emission lines originating from spatial details as small as 1 arc sec. In addition, the spectrograph slit covers a full solar radius simultaneously with approximately 1000 resolution elements. This allows the slit to be placed in such a way that it covers many different solar features at the same time (quiet Sun, plages, sunspots, center-to-limb variation). One spectrum contains enough information for a meaningful statistical analysis.

The major observing technique on Spacelab 2 will be the photographing of series of spectra over a period of at least 15 min to follow the changes in intensity, Doppler velocities, and line profiles as they are caused by disturbances moving through the solar atmosphere. The secondary observing technique will construct two-dimensional spectroheliograms as a function of time to investigate the three-dimensional structure of the chromosphere and transition zone. In addition, a systematic mapping of the coronal velocity field over the whole Sun will be made together with a series of limb spectra at different altitudes which will be used to study the structure and dynamics of spicules.

The study of intensity fluctuations, Doppler shifts, and line profile changes is crucial for the understanding of the mechanism that is responsible for the heating of the chromosphere, transition zone, and corona. However, so that definitive conclusions concerning the physical nature of the observed phenomena can be reached, it is required that the slit of the spectrograph be kept pointed within a tolerance of half a slit width on the solar surface for a duration of at least 15 min to observe disturbances propagating from the temperature minimum into the transition zone. Only a time series of spectra will reveal temperature and density changes as a function of time and altitude. Therefore, the combination of time sequences with the simultaneous coverage of many lines originating from different temperature regimes is necessary to reveal the propagation of disturbances through the solar atmosphere.

The second observing technique follows from the results of rocket flight experiments which indicate that the chromospheric and transition zone fine structure does not necessarily follow vertical columns. If only one-dimensional spectra are taken, it is not possible to follow disturbances that have a lateral movement. The HRTS instrument has a provision to step the slit between exposures in rapid sequence over a small area of the Sun (±10 arc sec). If this procedure is repeated many times over a

time period of 15 min, not only can spectroheliograms of different layers of the solar atmosphere be constructed, but also the change of line profiles and Doppler motions over a two-dimensional area can be investigated. This will reveal the static and dynamic three-dimensional fine structure.

The HRTS instrumentation consists of a telescope, an ultraviolet spectrograph, an ultraviolet spectroheliograph, and an H-alpha slit display system, all housed in a thermal control canister mounted on the Instrument Pointing System (IPS). The experiment is shown schematically in Figure X-1. The electronics control package is housed in a second canister on the IPS. An optical schematic is shown in Figure X-2, and the experiment hardware is shown in Figure X-3.

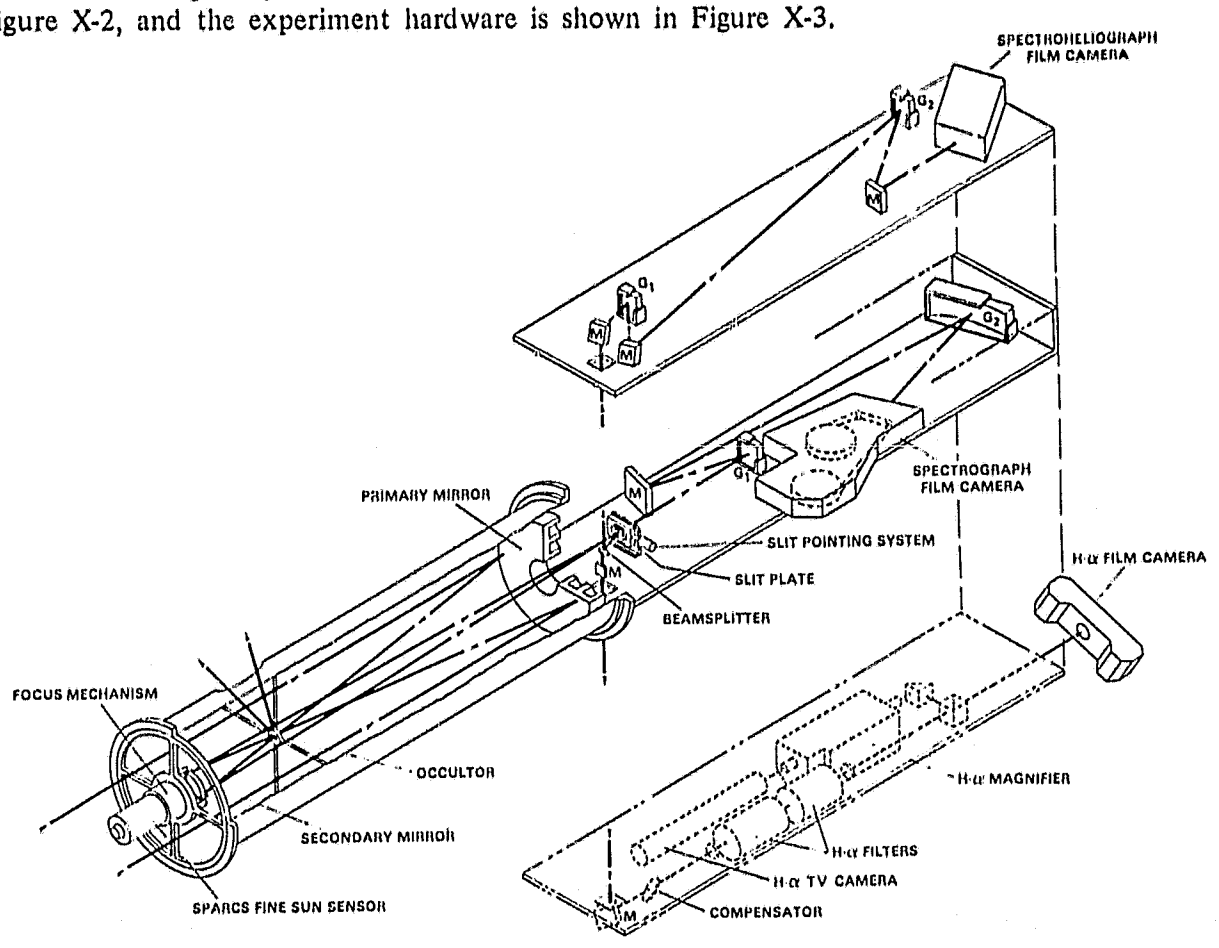

Figure X-1. Schematic view of the High Resolution Telescope and Spectrograph (HRTS).

The telescope is a concentric Gregorian in which the final image is formed on the telescope axis. The primary mirror is a 30-cm diameter paraboloid with 90-cm focal length. An occulting mirror located at the primary mirror focus reflects away all but a 7 X 15 arc min portion of the solar image. This 7 X 15 arc min portion passes through an aperture in the occulting mirror and strikes the secondary mirror which re-images it at the ultraviolet spectrograph slit plate. The focal lengths and occulting mirror aperture size have been arranged so that the secondary mirror is illuminated with only 1.5 solar constants, thus minimizing the problems of overheating and contamination of the secondary mirror. The telescope resolution is diffraction limited at 0.5 arc sec.

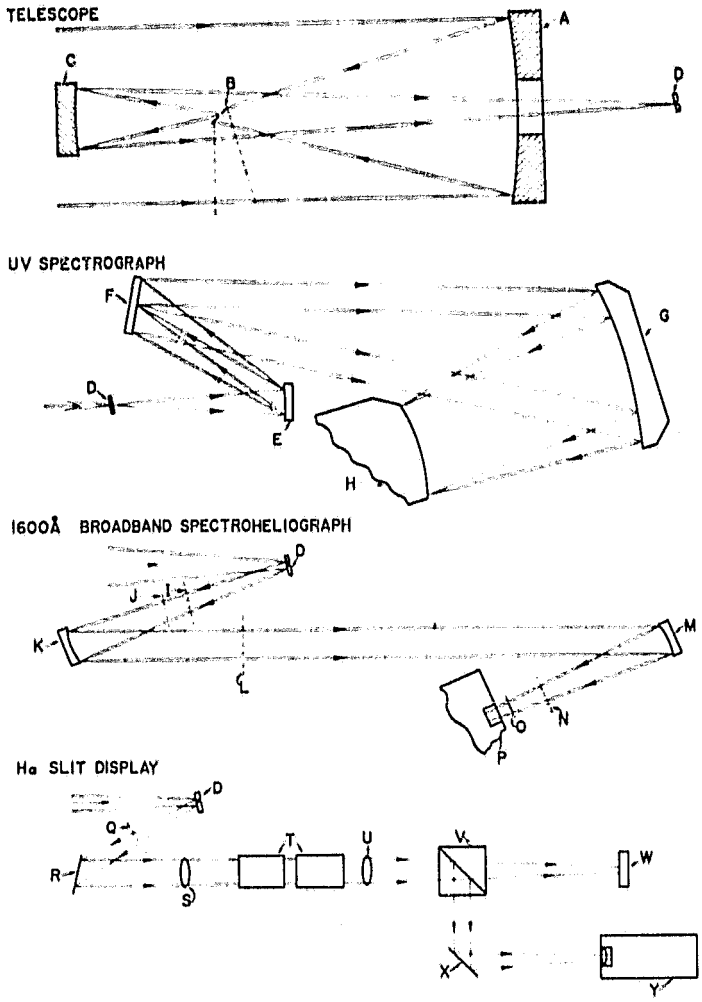

Figure X-2. Optical schematic of experiment.

The ultraviolet spectrograph is of the symmetric tandem Wadsworth type, using two concave diffraction gratings of equal radius and ruling density. A stigmatic spectrum with a spectral resolution of 50 mÅ and a spatial resolution of 0.5 arc sec everywhere along the slit length is formed at the film camera. A roll film camera holds 1000 exposures of Type SO 652 film.

The ultraviolet spectroheliograph instrument photographs the solar image reflected from the front surface of the spectrograph slit plate. It is tuned to observe the Carbon IV emission lines at 1550 Å which are formed in the solar transition zone. This instrument is a reversed tandem Wadsworth arrangement using two concave gratings which form a zero-dispersion image at the camera focal plane. The bandpass has a halfwidth of 35 Å (FWHM) and is controlled by the limited illumination of the second grating and a spike filter in front of the camera. The spatial resolution is 1.0 arc sec over the 5 X 15 min field of view.

The H-alpha slit display system forms a photographic and video image of the solar image reflected from the front surface of the spectrograph slit plate, filtered at 6563 Å. The H-alpha filter consists of two tandem, Fabry-Perot interference filters having a halfwidth of 0.5 Å. The final image is divided by a beamsplitter and imaged onto the focal planes of a modified Nikon camera using type

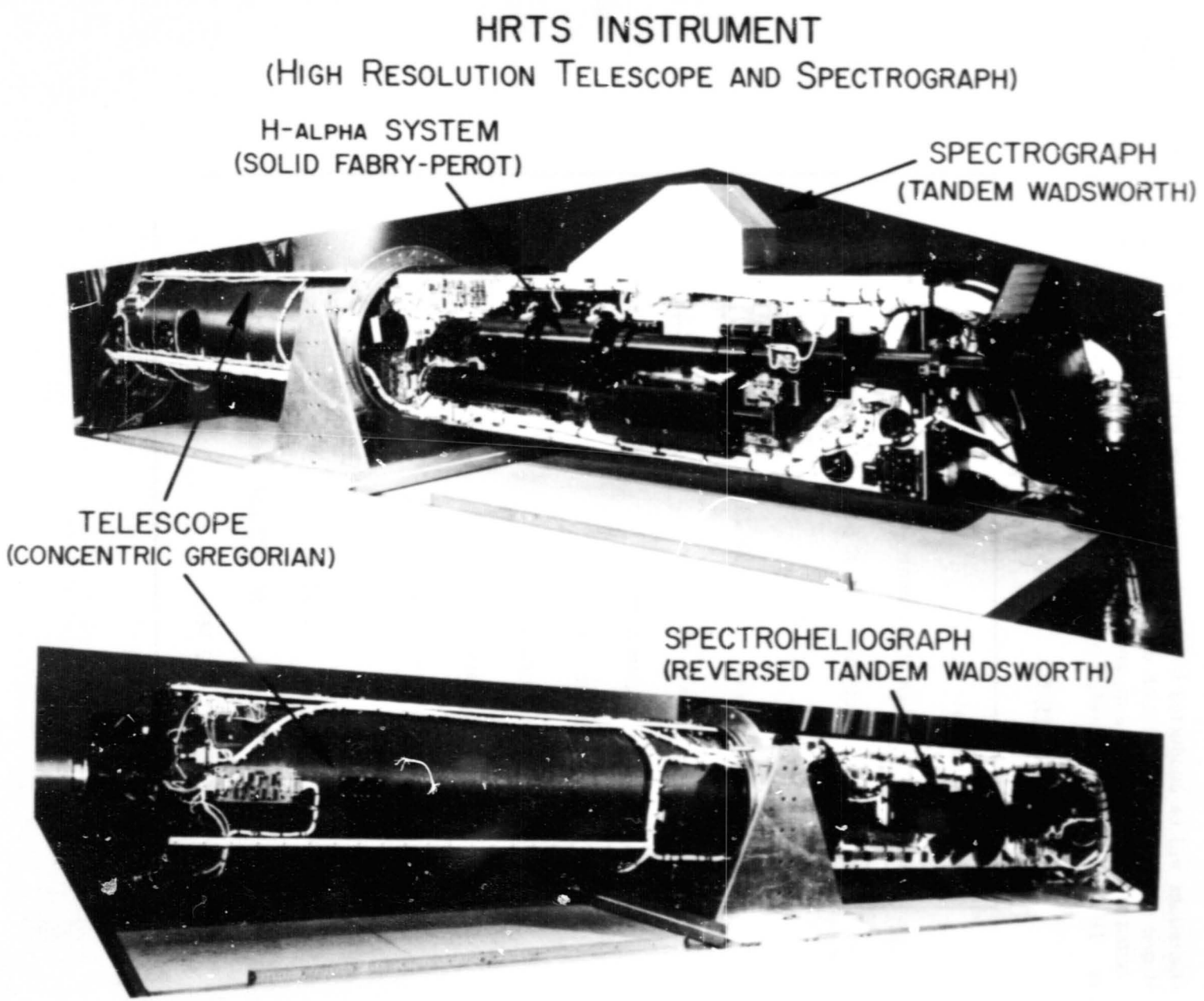

Figure X-3. Experiment hardware for the High Resolution Telescope and Spectrograph.

SO-410 film and a Westinghouse low-light-level MINSIT camera. The TV image is used in flight by the payload specialist to focus the telescope and to align solar features of interest onto the spectrograph slit.

Operations will be conducted in a single point mode with the slit of the spectrograph positioned at one stationary solar location during the exposure sequence, a rastering mode with the slit stepped across a segment of the Sun, and a limb scan mode for on-limb and off-limb exposure sequences. The physical characteristics of the overall experiment are listed in Table X-1.

TABLE X-1. PHYSICAL CHARACTERISTICS

Dimensions:
HRTS Instrument: 49 cm Dia X 365 cm (Pallet-IPS)
Electronics: 49 X 60 cm (Pallet-IPS)
Total Mass: 326 kg
Average Power: 340 W at 28 Vdc
Total Energy: 48.6 kWh
Pointing Requirements:
Mount: IPS
Orientation: Solar
Accuracy: 60 arc sec
Stability: 1 arc sec
Data:
Digital: 3.2 kbps
Film: Type SO-652 and Type SO-410
TV: 4.2 MHz

XI. SOLAR UV SPECTRAL IRRADIANCE MONITOR (SUSIM) (2SL-11)

Guenter Brueckner
Naval Research Laboratory

Many different layers of the solar atmosphere from the photosphere into the transition zone emit radiation in the 120- to 400-nm wavelength band. Similarly, this radiation is absorbed over a wide altitude range (0 to 130 km) in the terrestrial atmosphere, contributing to atmospheric effects. An accurate knowledge of the Sun's output and its variability in this wavelength range is necessary for a better understanding of solar-terrestrial phenomena.

Measurements made to date in this wavelength range have established absolute solar fluxes within ±30 percent in the 140- to 210-nm region, with better accuracy at longer wavelengths. However, these measurements are not accurate enough to establish credible values for long-term variations of the solar flux. The amplitude of these variations will cover several orders of magnigude from an indetectable 0.1 percent in the photospheric continuum at 400 nm to more than 100 percent in strong emission lines originating in the upper chromosphere and transition zone.

The observations of the Solar UV Spectral Irradiance Monitor (SUSIM) experiment have a threefold general objective: (1) to improve the accuracy of knowledge of the absolute solar fluxes, (2) to provide a highly accurate traceability of solar fluxes to a variety of ultraviolet radiation standards to be able to establish long-term (solar cycle) variations, and (3) to measure the variability of solar fluxes during several different time periods ranging from flare-produced changes to the variability caused by solar rotation. Specifically, the main objective of the measurements is to establish solar ultraviolet fluxes and their changes over a solar activity cycle in the wavelength region 120 to 400 nm. Of particular interest is the variability of the solar continuum in the 170- to 210-nm region, which is absorbed in the Schumann-Runge bands of the Earth's atmosphere. The specific experiment tasks are:

a) To improve the absolute accuracy of solar continuum irradiance measurements in the 120- to 400-nm region with a goal of ±6 to 10 percent (wavelength dependent).

b) To measure with high accuracy the intensities of the continuum below 208 nm relative to the intensities of the continuum above 208 nm with a goal of ±1 percent.

c) To perform high-accuracy measurements of the intensities of solar emission lines relative to the stable solar continuum above 208 nm with a goal of ±1 to 5 percent (wavelength dependent).

d) To improve the absolute accuracy of solar emission line irradiance measurements in the 120- to 400-nm region with a goal of ±6 to 10 percent (wavelength dependent).

A 7-day Space Shuttle flight obviously cannot solve the problems of the long-term variability. It is necessary to repeat such measurements over a solar cycle in time intervals of 1 year. To make these measurements comparable it is necessary that the highest possible calibration accuracy is applied to each flight and that the stability of the instrument is properly tracked during the mission.

To achieve this goal, a new approach will be used, with the main emphasis on improvements in three different areas: (1) improvement of existing calibration methods, (2) a new scheme of a strict environmental control of the instrument, and (3) and elaborate combination of in-flight calibration and redundant measuring methods to distinguish instrument changes from true solar flux variations.

The solar ultraviolet spectral irradiance monitor, shown in block diagram form in Figures XI-1 and XI-2, consists of two identical double-dispersion scanning spectrometers, seven detectors (five photodiodes and two photon counters), and an ultraviolet calibration light source. The spectrometers and detectors are sealed in a canister filled with 1.1 atm of argon to eliminate the effects of contamination due to high vacuum outgassing. Figure X-3 is a photograph of the experiment hardware.

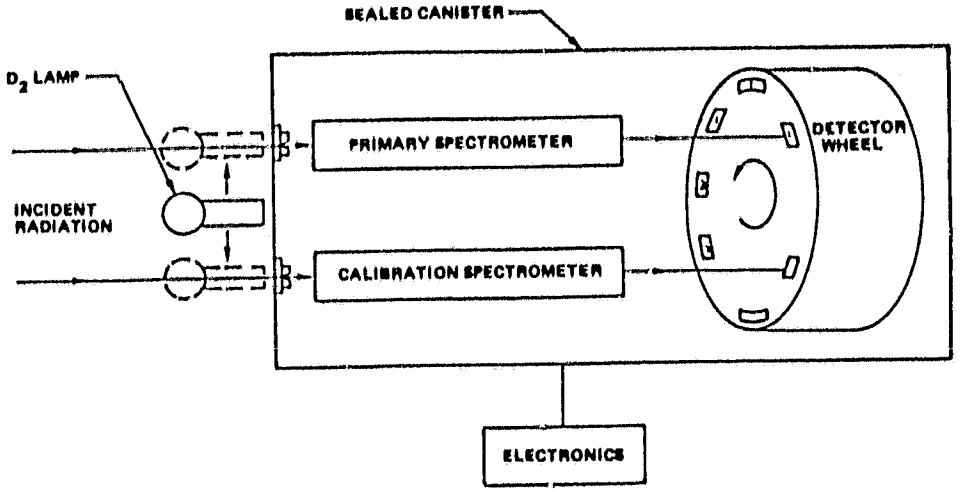

Figure XI-1. Block diagram for Solar UV Spectral Irradiance Monitor (SUSIM).

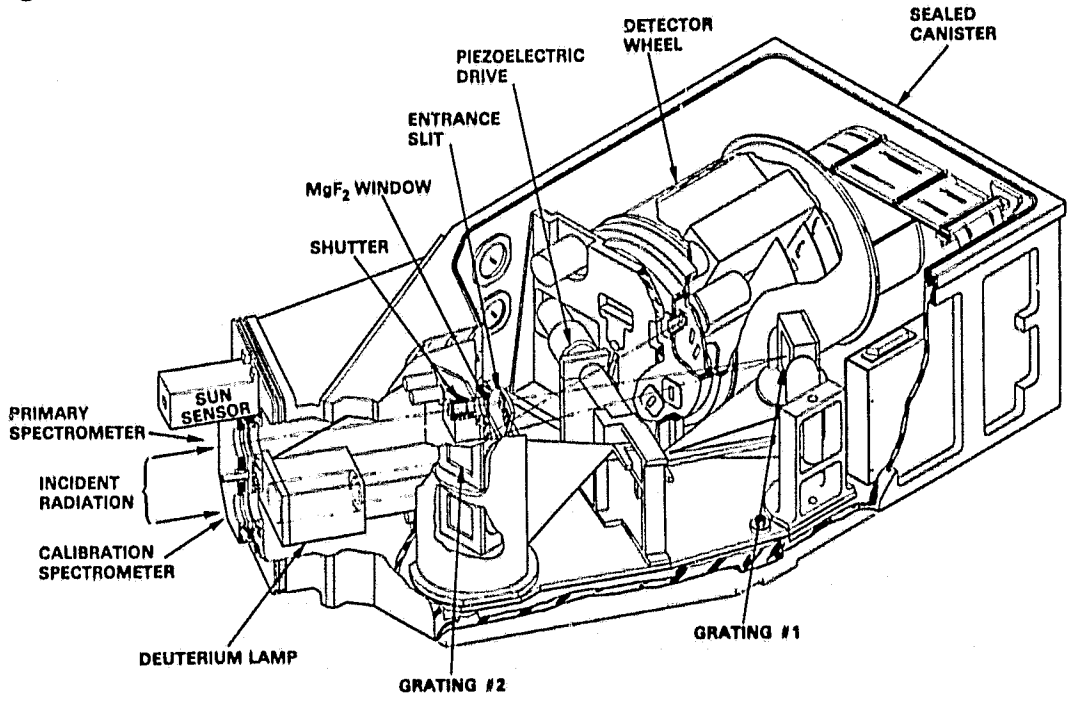

Figure XI-2. Representation of the Solar Ultraviolet Spectral Irradiance Monitor.

ORIGINAL PAGE
BLACK AND WHITE PHOTOGRAPH

Figure XI-3. Hardware for the SL2 Solar Ultraviolet Spectrai Irradiance Monitor experiment.

One spectrometer is used almost continuously during the daylight portion of each solar-pointed orbit to measure the short time variations of the solar ultraviolet flux (flare-related changes and the slowly varying component). The second spectrometer is used only once every day to track any change in sensitivity of the first spectrometer. Similarly, two of the five photodiodes are used only once every day.

A deuterium lamp, calibrated in spectral irradiance by the National Bureau of Standards (NBS), is used as the transfer standard source for daily in-flight calibration and stability tracking of both spectrometers and all seven detectors.

A spectral resolution of 0.15 nm over the entire wavelength range is obtained with two photon counters (operating in the stable pulse height discrimination mode), while 5-nm resolution is obtained with the five photodiodes (calibrated as transfer standard detectors by NBS). A microprocessor controls all instrument functions via program instruction.

The observational modes of the experiment include a continuous monitoring mode in which eight broad-band channels (5-nm resolution) will be monitored five times every solar-pointed orbit (total observing time 15 min). The channels are chosen to monitor the Lyman-alpha line at 121.6 nm and seven segments of the solar continuum, ranging from 145 to 390 nm. This mode is designed to measure the slowly varying component and continuum changes with high accuracy. During the remainder of each orbit, eight narrow-band channels (0.1-nm resolution) will be monitored continuously. The channels include five important solar emission lines scanned in five 0.1-nm steps and three continuum segments. This mode can detect with high resolution flare-related emission line changes and flux changes in emission lines caused by the slowly varying component. The continuum scans are necessary for reference calibration.

In spectral scan mode, which occurs once each day, the entire spectrum (120 to 400 nm) will be scanned with 0.1-nm resolution. This mode allows measurement of flux changes in all the remaining emission lines caused by the slowly varying component. Also, once every day, a calibration and stability tracking measurement will be made. In the narrow-band mode, a spectral scan of the solar spectrum and the deuterium lamp spectrum will be performed with each of the two spectrometers. In the broad-band mode, the eight channels will be monitored with each spectrometer, using the Sun and the deuterium lamp as the source. This mode is designed to determine instrument changes of the prime spectrometer and detectors and to measure long-term solar flux changes. To detect long-term ultraviolet flux variations it is necessary to determine, with high accuracy, changes in the instrument reflectivity and detector efficiency. It must be assumed that these changes are wavelength dependent. They can be determined using the Sun as a standard at 400 nm and the deuterium lamp's relative spectral output, which is known to be very stable.

The experiment will be mounted on the IPS. The physical characteristics of the experiment are shown in Table XI-1.

TABLE XI-1. PHYSICAL CHARACTERISTICS

Dimensions: 24 X 77 X 86 cm (Pallet-IPS)
Total Mass: 84 kg
Average Power: 74 W at 28 Vdc
Total Energy: 12 kWh
Pointing Requirements:
Mount: IPS
Orientation: Solar
Accuracy: 1800 arc sec
Stability: 360 arc sec
Data: 0.5 kbps

XII. PROPERTIES OF SUPERFLUID HELIUM IN ZERO-G
(2SL-12)

Peter V. Mason
Jet Propulsion Laboratory

Below the lambda point at 2.2 K, liquid helium enters the superfluid state. This state is characterized by near absence of energy dissipation below a critical velocity and very low dissipation at higher velocities, thermal conductivity about 1,000 times that of copper, existence of the temperature-induced fountain pressure, and the existence of wave mechanisms unknown in other fluids. This unique state has excited theoretical and experimental interest for many years. In addition, superfluid helium serves a technological function as a cryogen, and in the next few years it will find applications in space for far infrared astronomy missions; for cooling superconductive magnets, amplifiers, and computers; for cooling gyroscopes; for gravitational wave detectors; and for measurements of critical point phenomena.

Since superfluid helium is a liquid of anomalously low and nonlinear viscosity, its behavior is difficult to predict theoretically. Preliminary measurements have been performed in the laboratory, in short-term zero-g aircraft flights, and in sounding rockets. However, long-duration measurements in large volumes are essential to guide development of theory and to provide empirical engineering data for design of future space cryostat systems.

This experiment is designed to determine the fluid and thermal properties which will be required for the design of planned space experiments using superfluid helium as a cryogen, to advance scientific understanding of the interactions between superfluid and normal liquid helium, and to demonstrate the use of superfluid helium as a cryogen in zero gravity. Specifically, the objectives of the experiment are:

a) To make detailed measurements of low-frequency slosh modes of superfluid helium. For liquid helium in very low gravity conditions, weak surface tension forces determine the location of the fluid. As a result, large-amplitude, low-frequency sloshing motions of the bulk cryogen in response to external accelerations may be expected. These will generate mechanical forces which may displace the liquid to the point that thermal contact between the heat load and the cryogen is broken. Also, the bulk fluid motion may interact with sensitive experimental systems, e.g., gravity wave detectors. The sloshing amplitudes, frequencies, and damping must be known for future experiment design.

b) To make precise measurements of the thermal fluctuations and distributions in superfluid helium in zero-g. In superfluid helium in the laboratory, a degree of temperature uniformity of a few 10's of micro-Kelvins is found in space and time. Because most experiments utilizing liquid helium make use of this unique stability, it is necessary to evaluate the nonuniformities that the zero-g conditions and bulk-fluid motions induce. Quantitative measurements of spatial distributions and the spectrum of temporal fluctuations will be required by designers of future experiments. The purpose of this experiment is to perform such measurements at the micro-Kelvin level over a frequency range from 0 to 100 Hz.

c) To develop an apparatus to measure the velocities and attenuation of quantized surface waves in superfluid films in a regime of frequency at frequencies so high that surface tension forces dominate over gravity forces, and attenuation effects on Earth preclude their measurement.

d) To obtain superfluid helium cryostat performance data for future space applications. It is planned to measure temperature distributions and the spectrum of temperature fluctuations within the main helium dewar and pressures in vent control lines. These data are essential for the engineering analysis of the

development cryostat performance prior to its use in space science applications. The data will also be correlated with liquid location data obtained from the bulk fluid dynamics experiments to assess the effect of liquid location and to evaluate the limits of the effectiveness of the superfluid cryogen systems for space.

The experiment will consist of an instrumented cryostat (Figs. XIII-1 and XIII-2), an experiment package inside the cryostat, and a support electronics package. The experiment cavity is surrounded by a 100-liter superfluid helium volume and a multilayer super insulation system space by helium vapor cooled shields. External plumbing consists of fill and vent line systems located such that the dewar can operate in the upright and horizontal configurations. Valves will be used to direct and control flow for fill, vent, and porous plug operation. The cryostat will be instrumented with germanium and thermocouple temperature sensors to monitor the chamber temperatures and the superfluid plug and insulation performance. Accelerometers will monitor vibration effects to cross-correlate with the observations of bulk behavior.

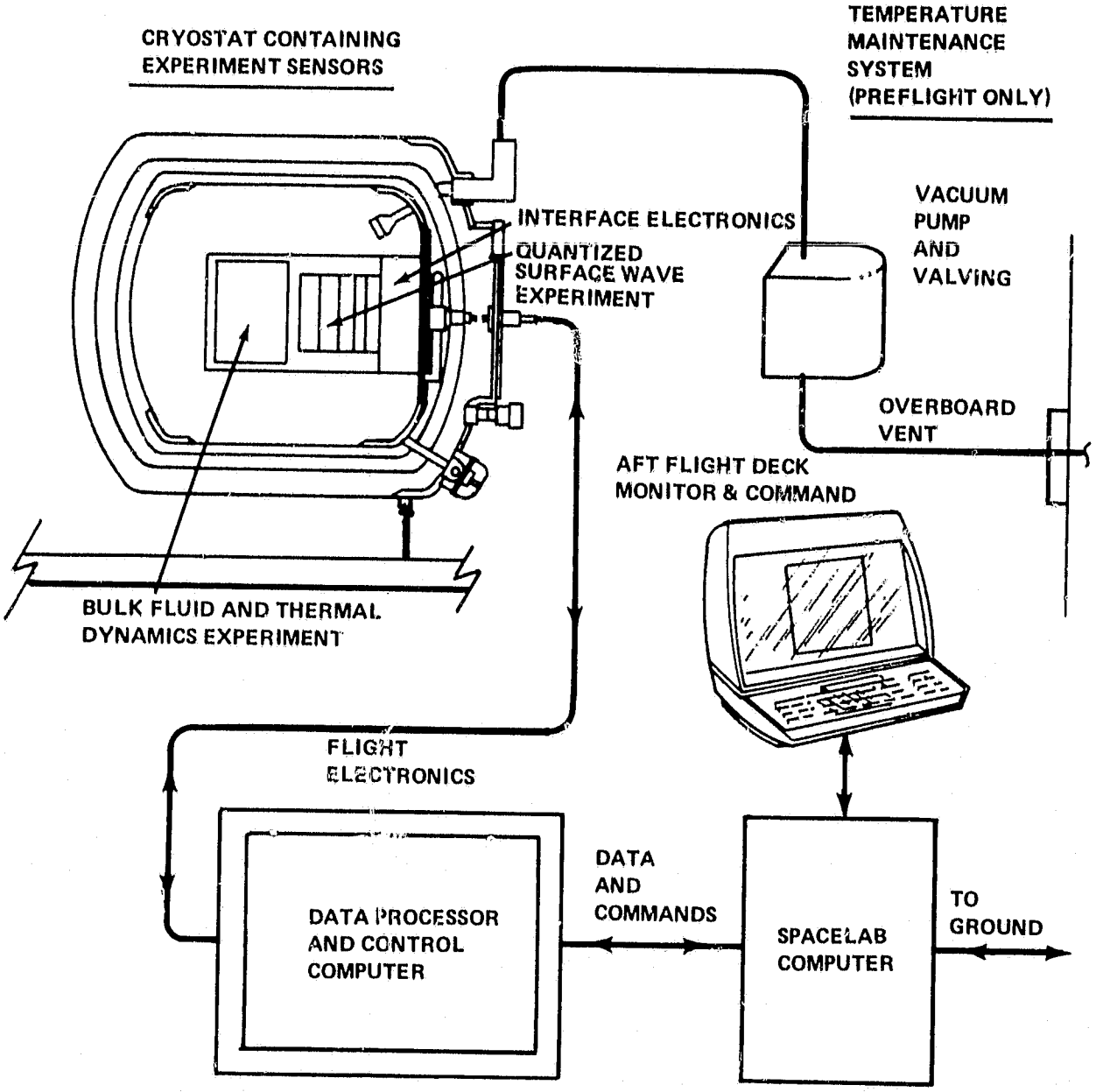

Figure XII-1. Spacelab 2 superfluid helium experiment.

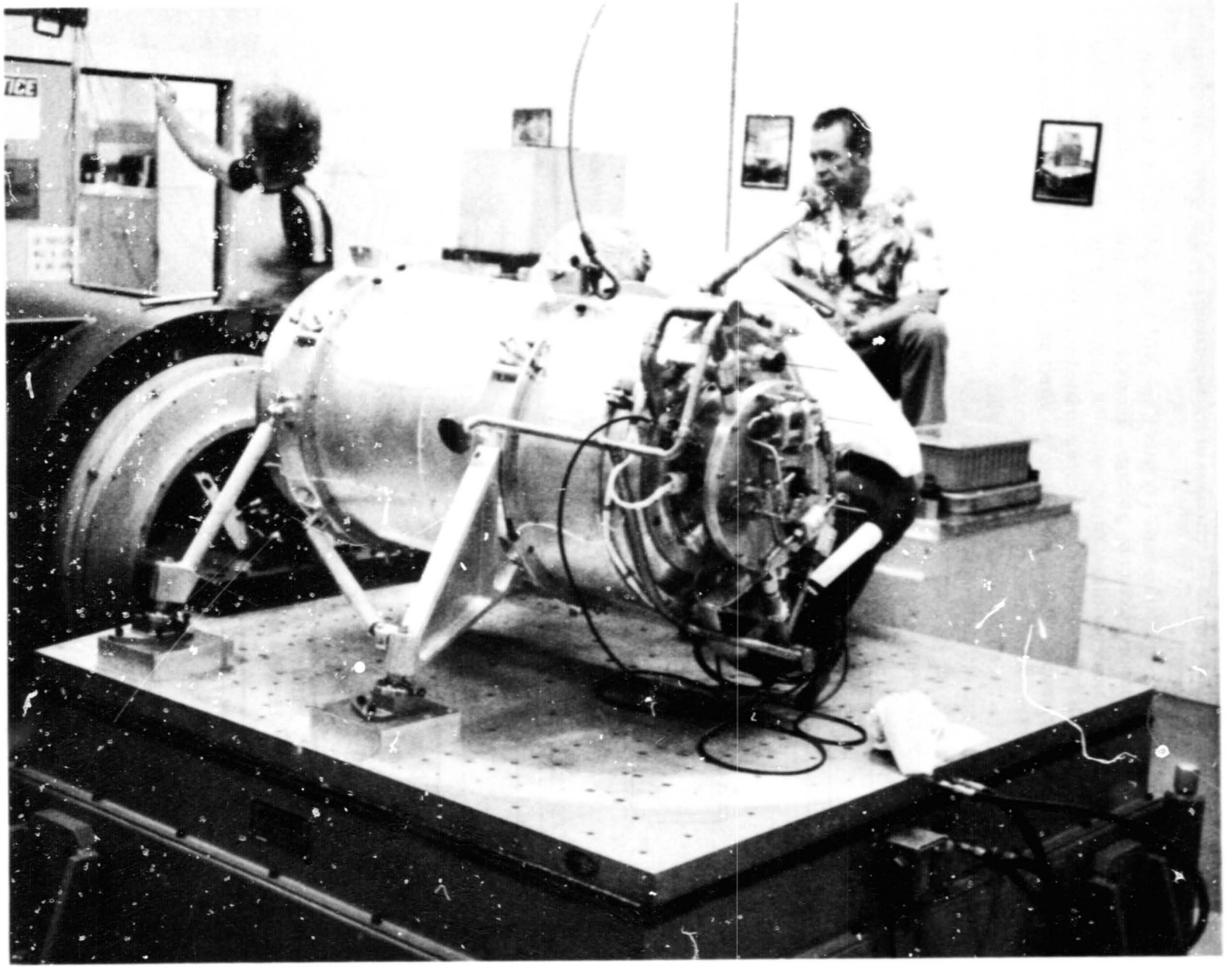

Figure XII-2. Cryostat assembly of the superfluid helium experiment for Spacelab Mission 2 being prepared for dynamic testing. Ball Aerospace Systems Division (BASD), Boulder, Colorado.

The experiment apparatus to be used to measure thermal and fluid dynamics will utilize an open-frame structure to position 133 liquid-vapor phase sensors in a 3-liter volume partially filled with liquid helium. The sensor outputs will be analyzed to yield maps of the liquid-vapor interface. Changes of this interface location will be correlated with accelerations derived from other instrumentation to determine fluid motion amplitude, frequency, and damping. The frame will also be instrumented with semiconductor thermometers to perform absolute and differential temperature measurements within the helium space. Thermal sensors of differing sensitivity and frequency response will be necessary to obtain the desired data on spatial distribution and the spectrum of the temporal variations. Spatial distribution of temperature will be measured by a network of 24 semiconductor sensors capable of resolving differences of 10 micro-Kelvin at frequencies up to 1 Hz. The spectrum of temperature fluctuations will be measured using eight carbon-film detectors of 1 milli-Kelvin sensitivity responding to frequencies from dc to 100 Hz.

In the quantized surface wave experiment, superfluid films will be contained in polished annual channels located in several sealed experiment chambers. Each chamber will have a different film thickness in the saturated range from 1 to 10 μm. A film heater will be placed in each channel to generate capillary waves in the film. The capillary wave will make repeated passes around the ring, giving a path length of $2\pi rn$, where r is the radius of the path and n is the number of times the pulse circulates. The relative thickness of the film and the amplitude of the capillary wave will be monitored by a capacitor capable of detecting small changes in thickness. Wave velocity and damping will be determined by measuring time and amplitude change of successive arrivals. Heater and sensor location will be chosen so that clockwise and counter-clockwise travelling waves do not arrive at the detector at the same time. It is expected that at least moderately accurate estimates of the velocity and attenuation of quantized surface waves in the capillary regime from 1 to 100 Hz in the films from 0.1 to 1 μm thickness will be obtained.

During flight operations, periods of low Orbiter activity (10^{-4} g) and high activity (10^{-3} g) will be used for data collection. Physical characteristics of the experiment are shown in Table XIII-1.

TABLE XII-1. PHYSICAL CHARACTERISTICS

Dimensions:

Cryostat: 75 cm Dia X 123 cm

Experiment Processor: 24 X 29 X 53 cm (Pallet)

Vacuum Pump: 30 X 30 X 45 cm (Pallet)

Total Mass: 250 kg

Average Power: 93 W at 28 Vdc
Total Energy: 14 kWh
Data: 20 kbps

APPENDIX

LIST OF CO-INVESTIGATORS

2SL-01 – VITAMIN D METABOLISM AND BONE DEMINERALIZATION

Dr. Hector F. DeLuca, University of Wisconsin
Dr. Emily Holton, Ames Research Center

2SL-02 – THE INTERACTION OF OXYGEN AND GRAVITY-INFLUENCED LIGNIFICATION

Dr. H. William Scheld, University of Houston

2SL-03 – AN EJECTABLE PLASMA DIAGNOSTICS PACKAGE

Dr. Louis A. Frank, University of Iowa
Dr. Donald A. Gurnett, University of Iowa
Dr. Nicola D' Angelo, University of Iowa
Dr. Nobie H. Stone, Marshall Space Flight Center
Dr. David L. Reasoner Marshall Space Flight Center
Mr. Henry Brinton, Goddard Space Flight Center
Mr. Dwight Fortna, Goddard Space Flight Center

2SL-04 – PLASMA DEPLETION EXPERIMENTS FOR IONOSPHERIC AND RADIO ASTRONOMICAL STUDIES

Dr. Michael D. Papagiannis, Boston University
Dr. R. A. Helliwell, Stanford University
Dr. M. Pongratz, University of California
Dr. G. Smith, University of California
Dr. D. J. Baker, Utah State University
Dr. R. Harris, Utah State University
Dr. D. Farley, Cornell University
Dr. M. Kelley, Cornell University
Dr. D. Anderson, NOAA

Additional Team Members

Dr. Jeffrey Forbes, Boston University
Dr. John V. Evans, MIT Lincoln Laboratory
Dr. Ron Wand, MIT Lincoln Laboratory
Mr. John A. Klobuchar, Air Force Geophysics Laboratory
Capt. Edward Weber, Air Force Geophysics Laboratory
Dr. Robert Eather, Boston College
Prof. G. A. R. Ellis, University of Tasmania

2SL-05 – A SMALL, HELIUM-COOLED INFRARED TELESCOPE

Dr. William F. Hoffmann, University of Arizona
Dr. Douglas E. Kleinmann, Smithsonian Astrophysical Observatory
Dr. Frank J. Low, University of Arizona
Dr. George H. Rieke, University of Arizona
Dr. Wesley A. Traub, Smithsonian Astrophysical Observatory
Dr. Eugene W. Urban, Marshall Space Flight Center

Associate Investigators

Dr. Fred C. Witteborn, Ames Research Center
Dr. Janet Simpson, Ames Research Center

Project Scientist

Dr. David G. Koch

2SL-06 – ELEMENTAL COMPOSITION AND ENERGY SPECTRA OF COSMIC RAY NUCLEI BETWEEN 50 GeV/NUCLEON AND SEVERAL TeV/NUCLEON

Mr. James E. Lamport, University of Chicago
Dr. Jacques L'Heureux, University of Chicago

2SL-07 – HARD X-RAY IMAGING OF CLUSTERS OF GALAXIES AND OTHER EXTENDED X-RAY SOURCES

Dr. David K. Bedford, University of Birmingham/U.K.
Dr. Geoffrey F. Carpenter, University of Birmingham/U.K.
Dr. Christopher J. Eyles, University of Birmingham/U.K.
Dr. John R. H. Herring, University of Birmingham/U.K.
Dr. George M. Simnett, University of Birmingham/U.K.
Dr. Gerald K. Skinner, University of Birmingham/U.K.
Dr. Joseph W. G. Wilson, University of Birmingham/U.K.

2SL-08 – A SOLAR MAGNETIC AND VELOCITY FIELD MEASUREMENT SYSTEM

Mr. Harry E. Ramsey, Lockheed Solar Observatory
Dr. Robert C. Smithson, Lockheed Solar Observatory
Dr. Stephen A. Schoolman, Lockheed Solar Observatory
Dr. Theodore D. Tarbell, Lockheed Solar Observatory
Dr. Loren W. Acton, Goddard Space Flight Center
Dr. John W. Harvey, Kitt Peak National Observatory
Dr. William L. Livingston, Kitt Peak National Observatory
Dr. Robert W. Milkey, Kitt Peak National Observatory
Dr. Jack B. Zirker, Air Force Geophysics Laboratory
Dr. George W. Simon, Air Force Geophysics Laboratory
Dr. Simon P. Worden, Air Force Geophysics Laboratory

2SL-09 – CORONAL HELIUM ABUNDANCE SPACELAB EXPERIMENT (CHASE)

Mr. B. E. Patchett, SRC Rutherford and Appleton Laboratory/U.K.
Mr. K. Strong, University College, London/U.K.
Mr. K. Norman, Mullard Space Science Laboratory/U.K.

2SL-10 – A HIGH RESOLUTION TELESCOPE AND SPECTROGRAPH

Dr. John-David F. Bartoe, Navel Research Laboratory
Mr. Kenneth R. Nicolas, Naval Research Laboratory
Dr. Olav Kjeldseth Moe, Naval Research Laboratory
Mr. Michael E. VanHoosier, Naval Research Laboratory
Dr. Carole Jordan, University of Oxford/U.K.

2SL-11 – SOLAR UV SPECTRAL IRRADIANCE MONITOR

Dr. John-David F. Bartoe, Naval Research Laboratory
Dr. Dianne K. Prinz, Naval Research Laboratory
Mr. Michael E. VanHoosier, Naval Research Laboratory

2SL-13 – PROPERTIES OF SUPERFLUID HELIUM IN ZERO-G

Dr. Donald J. Collins, Jet Propulsion Laboratory
Dr. Daniel D. Ellemen, Jet Propulsion Laboratory
Dr. Dusan Petrac, Jet Propulsion Laboratory
Dr. Melvin Saffren, Jet Propulsion Laboratory
Dr. Taylor Wang, Jet Propulsion Laboratory